

effective as a GJIC inhibitor in WB-F344 cells (Fig. 2B). We were aware that anisomycin might also act as a translational inhibitor at such concentrations. A previous study (Mahadevan and Edwards, 1991) has shown that relatively low concentrations of anisomycin (around 25–50 ng ml⁻¹; so-called subinhibitory levels) can selectively activate the p38 MAP kinase without inhibiting protein synthesis. In our study, however, even a lower concentration of anisomycin (10 ng ml⁻¹) appeared to have an ability to inhibit protein synthesis, but this concentration could not activate p38 MAP kinase (Fig. 2B, Fig. 3C). This discrepancy might be due to the different cell lines used in the studies. In any event, GJIC could be maintained at the control level by SB203580 pretreatment without recovery of protein synthesis (Fig. 5D), indicating that the effect of anisomycin on GJIC was not dependent on the inhibition of protein synthesis. Our conclusion gained further support from our observation that SB203580 pretreatment of the cells appeared to be capable of preventing anisomycin-induced losses of the P1 or P2 (but not P0) forms of Cx43. Moreover, both before and after treatment in our experiments, we checked the effects on the intracellular levels of ZO-1, occludin, E-cadherin and β -catenin as reference proteins, which have short half-lives like that of Cx43. We did not detect changes in the levels of these reference proteins in any anisomycin treatment experiment.

Anisomycin is also a well known inducer of apoptosis in other cell lines (Polverino and Patterson, 1997; Stadheim and Kucera, 2002). Furthermore, the up- or downregulation of GJIC has been reported in the apoptotic process (Wilson et al., 2000). However, in our experiment, at least up to 120 minutes, anisomycin did not induce apoptosis in WB-F344 cells (data not shown).

A key finding of our present study is that pretreatment of anisomycin-exposed WB-F344 cells with SB203580 appeared to inhibit both the redistribution of Cx43 derivatives and to ameliorate or prevent the disruption of GJIC that anisomycin would otherwise have provoked. It is also important that the protection against GJIC disruption afforded by SB203580 pretreatment was, for all intents and purposes, complete. Given that SB203580 is reputed to be a highly specific inhibitor of p38 MAP kinase (Cuenda et al., 1995; Tong et al., 1997), it seems likely that the most important single event in the anisomycin-induced disruption of GJIC involves its ability to activate this particular kinase. It remains uncertain whether our interpretation will turn out to be an oversimplification, if only because WB-F344 cells pretreated with SB203580 appear to experience virtually no disruption of GJIC under circumstances in which the inhibition of p38 MAP kinase by SB203580 is not complete. Moreover, western blotting analysis revealed that SB203580 was capable of inhibiting JNK and that inhibition of p38 MAP kinase was incomplete. These observations are in accordance with a report that SB203580 is capable of inhibiting JNK when used at relatively high concentrations (Clerk and Sugden, 1998) and others that SB203580 only appears to exert its inhibitory effect on specific isoforms of p38 MAP kinase (Cuenda et al., 1995; Lee et al., 1994). Suggestions that the p38 MAP kinase and JNK pathways engage in cross talk in response to anisomycin might also be relevant (Töröcsik and Szeberényi, 2000). We are currently conducting additional experiments in the hope of obtaining a more thorough understanding of the mechanisms involved in GJIC inhibition by the p38 MAP kinase pathway.

We thank Baxter Limited Renal Division for their support in conducting this study. This study was supported in part by Grants-in-Aid for Scientific Research from the Ministry of Education, Science, Sports and Culture of Japan, and for Cancer Research from the Ministry of Health and Welfare of Japan, and by a grant from the Smoking Research Foundation. We thank E. Suzaki (Department of Histology and Cell Biology, Hiroshima University School of Medicine, Hiroshima, Japan) and K. Yamashita (Department of Anatomy and Developmental Biology, Hiroshima University School of Medicine, Hiroshima, Japan) for helpful advice.

References

- Barros, L. F., Young, M., Saklatvala, J. and Baldwin, S. A. (1997). Evidence of two mechanisms for the activation of the glucose transporter GLUT1 by anisomycin: p38(MAP kinase) activation and protein synthesis inhibition in mammalian cells. *J. Physiol.* **504**, 517–525.
- Berthoud, V. M., Rook, M. B., Traub, O., Hertzberg, E. L. and Sáez, J. C. (1993). On the mechanisms of cell uncoupling induced by a tumor promoter phorbol ester in clone 9 cells, a rat liver epithelial cell line. *Eur. J. Cell Biol.* **62**, 384–396.
- Beyer, E. C., Paul, D. L. and Goodenough, D. A. (1987). Connexin43: a protein from rat heart homologous to a gap junction protein from liver. *J. Cell Biol.* **105**, 2621–2629.
- Cano, E., Hazzalin, C. A. and Mahadevan, L. C. (1994). Anisomycin-activated protein kinases p45 and p55 but not mitogen-activated protein kinases ERK-1 and -2 are implicated in the induction of c-Fos and c-Jun. *Mol. Cell Biol.* **14**, 7352–7362.
- Cano, E. and Mahadevan, L. C. (1995). Parallel signal processing among mammalian MAPKs. *Trends Biochem. Sci.* **20**, 117–122.
- Cho, J. H., Cho, S. D., Hu, H., Kim, S. H., Lee, S. K., Lee, Y. S. and Kang, K. S. (2002). The roles of ERK1/2 and p38 MAP kinases in the preventive mechanisms of mushroom *Phellinus linteus* against the inhibition of gap junctional intercellular communication by hydrogen peroxide. *Carcinogenesis* **23**, 1163–1169.
- Clerk, A. and Sugden, P. H. (1998). The p38-MAPK inhibitor, SB203580, inhibits cardiac stress-activated protein kinases/c-Jun N-terminal kinases (SAPKs/JNKs). *FEBS Lett.* **426**, 93–96.
- Cuenda, A., Rouse, J., Doza, Y. N., Meier, R., Cohen, P., Gallagher, T. F., Young, P. R. and Lee, J. C. (1995). SB 203580 is a specific inhibitor of a MAP kinase homologue which is stimulated by cellular stresses and interleukin-1. *FEBS Lett.* **364**, 229–233.
- Dupont, E., el Aoumari, A., Fromaget, C., Briand, J. P. and Gros, D. (1991). Affinity purification of a rat-brain junctional protein, connexin 43. *Eur. J. Biochem.* **200**, 263–270.
- Elvira, M., Diez, J. A., Wang, K. K. and Villalobo, A. (1993). Phosphorylation of connexin-32 by protein kinase C prevents its proteolysis by mu-calpain and m-calpain. *J. Biol. Chem.* **268**, 14294–14300.
- Girão, H. and Pereira, P. (2003). Phosphorylation of connexin 43 acts as a stimuli for proteasome-dependent degradation of the protein in lens epithelial cells. *Mol. Vis.* **9**, 24–30.
- Guan, X. and Ruch, R. J. (1996). Gap junction endocytosis and lysosomal degradation of connexin43-P2 in WB-F344 rat liver epithelial cells treated with DDT and lindane. *Carcinogenesis* **17**, 1791–1798.
- Hazzalin, C. A., le Panse, R., Cano, E. and Mahadevan, L. C. (1998). Anisomycin selectively desensitizes signalling components involved in stress kinase activation and Fos and Jun induction. *Mol. Cell Biol.* **18**, 1844–1854.
- Helliwell, P. A., Richardson, M., Affleck, J. and Kellett, G. L. (2000). Regulation of GLUT5, GLUT2 and intestinal brush-border fructose absorption by the extracellular signal-regulated kinase, p38 mitogen-activated kinase and phosphatidylinositol 3-kinase intracellular signalling pathways: implications for adaptation to diabetes. *Biochem. J.* **350**, 163–169.
- Hii, C. S., Ferrante, A., Edwards, Y. S., Huang, Z. H., Hartfield, P. J., Rathjen, D. A., Poulos, A. and Murray, A. W. (1995a). Activation of mitogen-activated protein kinase by arachidonic acid in rat liver epithelial WB cells by a protein kinase C-dependent mechanism. *J. Biol. Chem.* **270**, 4201–4204.
- Hii, C. S., Ferrante, A., Schmidt, S., Rathjen, D. A., Robinson, B. S., Poulos, A. and Murray, A. W. (1995b). Inhibition of gap junctional communication by polyunsaturated fatty acids in WB cells: evidence that connexin 43 is not hyperphosphorylated. *Carcinogenesis* **16**, 1505–1511.
- Hossain, M. Z., Ao, P. and Boynton, A. L. (1998a). Platelet-derived growth

- factor-induced disruption of gap junctional communication and phosphorylation of connexin43 involves protein kinase C and mitogen-activated protein kinase. *J. Cell Physiol.* **176**, 332-341.
- Hossain, M. Z., Ao, P. and Boynton, A. L. (1998b). Rapid disruption of gap junctional communication and phosphorylation of connexin43 by platelet-derived growth factor in T51B rat liver epithelial cells expressing platelet-derived growth factor receptor. *J. Cell Physiol.* **174**, 66-77.
- Hossain, M. Z., Jagdale, A. B., Ao, P. and Boynton, A. L. (1999a). Mitogen-activated protein kinase and phosphorylation of connexin43 are not sufficient for the disruption of gap junctional communication by platelet-derived growth factor and tetradecanoylphorbol acetate. *J. Cell Physiol.* **179**, 87-96.
- Hossain, M. Z., Jagdale, A. B., Ao, P., Kazlauskas, A. and Boynton, A. L. (1999b). Disruption of gap junctional communication by the platelet-derived growth factor is mediated via multiple signaling pathways. *J. Biol. Chem.* **274**, 10489-10496.
- Kanemitsu, M. Y. and Lau, A. F. (1993). Epidermal growth factor stimulates the disruption of gap junctional communication and connexin43 phosphorylation independent of 12-O-tetradecanoylphorbol 13-acetate-sensitive protein kinase C: the possible involvement of mitogen-activated protein kinase. *Mol. Biol. Cell* **4**, 837-848.
- Kyriakis, J. M., Banerjee, P., Nikolakaki, E., Dai, T., Rubie, E. A., Ahmad, M. F., Avruch, J. and Woodgett, J. R. (1994). The stress-activated protein kinase subfamily of c-Jun kinases. *Nature* **369**, 156-160.
- Laird, D. W., Castillo, M. and Kasprzak, L. (1995). Gap junction turnover, intracellular trafficking, and phosphorylation of connexin43 in bromfield A-treated rat mammary tumor cells. *J. Cell Biol.* **131**, 1193-1203.
- Lau, A. F., Kanemitsu, M. Y., Kurata, W. E., Danesh, S. and Boynton, A. L. (1992). Epidermal growth factor disrupts gap-junctional communication and induces phosphorylation of connexin43 on serine. *Mol. Biol. Cell* **3**, 865-874.
- Lee, J. C., Laydon, J. T., McDonnell, P. C., Gallagher, T. F., Kumar, S., Green, D., McNulty, D., Blumenthal, M. J., Heys, J. R., Landvatter, S. W. et al. (1994). A protein kinase involved in the regulation of inflammatory cytokine biosynthesis. *Nature* **372**, 739-746.
- Loewenstein, W. R. (1990). Cell-to-cell communication and the control of growth. *Am. Rev. Respir. Dis.* **142**, S48-S53.
- Mahadevan, L. C. and Edwards, D. R. (1991). Signalling and superinduction. *Nature* **349**, 747-748.
- Matesic, D. F., Rupp, H. L., Bonney, W. J., Ruch, R. J. and Trosko, J. E. (1994). Changes in gap-junction permeability, phosphorylation, and number mediated by phorbol ester and non-phorbol-ester tumor promoters in rat liver epithelial cells. *Mol. Carcinog.* **10**, 226-236.
- Minden, A. and Karin, M. (1997). Regulation and function of the JNK subgroup of MAP kinases. *Biochim. Biophys. Acta* **1333**, F85-F104.
- Musil, L. S., Cunningham, B. A., Edelman, G. M. and Goodenough, D. A. (1990). Differential phosphorylation of the gap junction protein connexin43 in junctional communication-competent and -deficient cell lines. *J. Cell Biol.* **111**, 2077-2088.
- Musil, L. S. and Goodenough, D. A. (1991). Biochemical analysis of connexin43 intracellular transport, phosphorylation, and assembly into gap junctional plaques. *J. Cell Biol.* **115**, 1357-1374.
- Musil, L. S. and Goodenough, D. A. (1993). Multisubunit assembly of an integral plasma membrane channel protein, gap junction connexin43, occurs after exit from the ER. *Cell* **74**, 1065-1077.
- Ogawa, T., Hayashi, T., Kyoizumi, S., Ito, T., Trosko, J. E. and Yorioka, N. (1999). Up-regulation of gap junctional intercellular communication by hexamethylene bisacetamide in cultured human peritoneal mesothelial cells. *Lab. Invest.* **79**, 1511-1520.
- Ogawa, T., Hayashi, T., Yorioka, N., Kyoizumi, S. and Trosko, J. E. (2001). Hexamethylene bisacetamide protects peritoneal mesothelial cells from glucose. *Kidney Int.* **60**, 996-1008.
- Polontchouk, L., Ebel, B., Jackels, M. and Dhein, S. (2002). Chronic effects of endothelin 1 and angiotensin II on gap junctions and intercellular communication in cardiac cells. *FASEB J.* **16**, 87-89.
- Polverino, A. J. and Patterson, S. D. (1997). Selective activation of caspases during apoptotic induction in HL-60 cells. Effects of a tetrapeptide inhibitor. *J. Biol. Chem.* **272**, 7013-7021.
- Ruch, R. J., Trosko, J. E. and Madhukar, B. V. (2001). Inhibition of connexin43 gap junctional intercellular communication by TPA requires ERK activation. *J. Cell Biochem.* **83**, 163-169.
- Seger, R. and Krebs, E. G. (1995). The MAPK signaling cascade. *FASEB J.* **9**, 726-735.
- Stadheim, T. A. and Kucera, G. L. (2002). c-Jun N-terminal kinase/stress-activated protein kinase (JNK/SAPK) is required for mitoxantrone- and anisomycin-induced apoptosis in HL-60 cells. *Leukocyte Res.* **26**, 55-65.
- Tong, L., Pav, S., White, D. M., Rogers, S., Crane, K. M., Cywin, C. L., Brown, M. L. and Pargellis, C. A. (1997). A highly specific inhibitor of human p38 MAP kinase binds in the ATP pocket. *Nat. Struct. Biol.* **4**, 311-316.
- Töröcsik, B. and Szeberényi, J. (2000). Anisomycin uses multiple mechanisms to stimulate mitogen-activated protein kinases and gene expression and to inhibit neuronal differentiation in PC12 pheochromocytoma cells. *Eur. J. Neurosci.* **12**, 527-532.
- Trosko, J. E., Chang, C. C., Wilson, M. R., Upham, B., Hayashi, T. and Wade, M. (2000). Gap junctions and the regulation of cellular functions of stem cells during development and differentiation. *Methods* **20**, 245-264.
- Trosko, J. E. and Ruch, R. J. (1998). Cell-cell communication in carcinogenesis. *Front. Biosci.* **3**, 208-236.
- Tsao, M. S., Smith, J. D., Nelson, K. G. and Grisham, J. W. (1984). A diploid epithelial cell line from normal adult rat liver with phenotypic properties of 'oval' cells. *Exp. Cell Res.* **154**, 38-52.
- Wade, M. H., Trosko, J. E. and Schindler, M. (1986). A fluorescence photobleaching assay of gap junction-mediated communication between human cells. *Science* **232**, 525-528.
- Warn-Cramer, B. J., Cottrell, G. T., Burt, J. M. and Lau, A. F. (1998). Regulation of connexin-43 gap junctional intercellular communication by mitogen-activated protein kinase. *J. Biol. Chem.* **273**, 9188-9196.
- Warn-Cramer, B. J., Lampe, P. D., Kurata, W. E., Kanemitsu, M. Y., Loo, L. W., Eckhart, W. and Lau, A. F. (1996). Characterization of the mitogen-activated protein kinase phosphorylation sites on the connexin-43 gap junction protein. *J. Biol. Chem.* **271**, 3779-3786.
- Wilson, M. R., Close, T. W. and Trosko, J. E. (2000). Cell population dynamics (apoptosis, mitosis, and cell-cell communication) during disruption of homeostasis. *Exp. Cell Res.* **254**, 257-268.

Caspase-2 and Caspase-7 Are Involved in Cytolethal Distending Toxin-Induced Apoptosis in Jurkat and MOLT-4 T-Cell Lines

Masaru Ohara,¹ Tomonori Hayashi,² Yoichiro Kusunoki,² Mutsumi Miyauchi,³
Takashi Takata,³ and Motoyuki Sugai^{1*}

Departments of Bacteriology¹ and Oral Maxillofacial Pathology,³ Hiroshima University Graduate School of Biomedical Sciences, Hiroshima 734-8553, and Department of Radiobiology and Molecular Epidemiology, Radiation Effects Research Foundation, Hiroshima 732-0815,² Japan

Received 20 May 2003/Returned for modification 12 August 2003/Accepted 22 October 2003

Cytolethal distending toxin (CDT) from *Actinobacillus actinomycetemcomitans* is a G₂/M cell-cycle-specific growth-inhibitory toxin that leads to target cell distension followed by cell death. To determine the mechanisms by which *A. actinomycetemcomitans* CDT acts as an immunosuppressive factor, we examined the effects of highly purified CDT holotoxin on human T lymphocytes. Purified CDT was cytolethal toward normal peripheral T lymphocytes that were activated by in vitro stimulation with phytohemagglutinin. In addition, purified CDT showed cytolethal activity against Jurkat and MOLT-4 cells, which are known to be sensitive and resistant, respectively, to Fas-mediated apoptosis. Death in these cell lines was accompanied by the biochemical features of apoptosis, including membrane conformational changes, intranucleosomal DNA cleavage, and an increase in caspase activity in the cells. Pretreatment of Jurkat cells with the general caspase inhibitor z-VAD-fmk mostly suppressed CDT-induced apoptosis. Furthermore, specific inhibitors of caspase-2 and -7 showed significant inhibitory effects on CDT-induced apoptosis in Jurkat cells, and these inhibitory effects were fully associated with reduced activity of caspase-2 or -7 in the CDT-treated Jurkat cells. These results strongly suggest that CDT possesses the ability to induce human T-cell apoptosis through activation of caspase-2 and -7.

Bacterial infections in mammals evoke a series of immune reactions to bacterial antigens in the infected host, but immune responses are occasionally suppressed or shut down by some bacterial products, such as toxins. Suppression or inactivation of the host immune response is considered to be a bacterial strategy to evade host immune mechanisms. *Actinobacillus actinomycetemcomitans* is a gram-negative rod-shaped pathogen implicated in the pathogenesis of juvenile and adult periodontitis (38). Previous studies demonstrated that *A. actinomycetemcomitans* produces a factor(s) that is immunosuppressive for human T and B cells (25). It was recently established that *A. actinomycetemcomitans* produces a new member of the cytolethal distending toxin (CDT) family which was previously unrecognized as a virulence factor of *A. actinomycetemcomitans* (40). CDT belongs to the family of toxins with cell-cycle-specific inhibitory activities which block the progression of cells from G₂ to M phase (28). CDT-poisoned cells undergo cell distension and nucleus swelling and eventually die. CDT was found to form a complex of three subunits, CDTA, -B, and -C (9, 14, 21, 24, 31, 40), and the subunits were determined to be tandemly encoded by the *cdtA*, *cdtB*, and *cdtC* genes at the chromosomal *cdt* loci. *A. actinomycetemcomitans* CDTA, -B, and -C are translated as approximately 25-, 32-, and 21-kDa proteins, respectively, and are secreted into the periplasm (40). After cleavage of their 15- to 21-amino-acid signal sequences at the N terminus, they become 23-, 29-, and 19-kDa proteins, respectively (31, 36, 40). CDTA goes through another process-

ing step to become an 18- to 19-kDa form, designated CDTA', and forms a complex with CDTB and CDTC to become a holotoxin (40).

In 1999, Shenker et al. purified the immunosuppressive factor of *A. actinomycetemcomitans* that could affect human T cells and demonstrated that the factor was one of the subunit proteins of CDT, CDTB (34, 36). Their group also demonstrated that a crude CDT preparation of *A. actinomycetemcomitans* induced cell cycle arrest at the G₂ phase in human peripheral blood cells (37). Furthermore, the CDT preparation was shown to induce apoptotic cell death in peripheral blood lymphocytes along with activation of caspase-3, -8, and -9 (35). Despite those findings, whether these caspases are really involved in CDT-induced apoptosis remains virtually unknown.

For this study, we studied the immunosuppressive effect of highly purified *A. actinomycetemcomitans* CDT on normal human T lymphocytes and made an in-depth characterization of the cytolethal effect by using the T-cell leukemia cell lines Jurkat and MOLT-4, which are sensitive and resistant, respectively, to Fas-mediated apoptosis. We herein demonstrate that CDT induces apoptosis in these cells and that caspase-2 and -7 play important roles in the signaling pathway of CDT-induced cell death, which is distinct from Fas-mediated apoptosis.

MATERIALS AND METHODS

Purification of *A. actinomycetemcomitans* CDT. CDT holotoxin was prepared by using the pQE 60 (C-terminal histidine tag) protein expression system in M15 *Escherichia coli* (Qiagen, Tokyo, Japan). Briefly, for construction of pQEcdtABC, the *A. actinomycetemcomitans* *cdtABC* gene was isolated from *A. actinomycetemcomitans* genomic DNA by PCR amplification with specific primers that contained several restriction enzyme sites for subcloning into vectors, as follows: QIA-U, 5'-AGGTACCATGGAAAAGTTT-3', which corresponds to the *cdtA* starting site with a *NcoI* restriction enzyme site; QIC-L, 5'-AAAGATCTGCT ACCCTGA-3', which corresponds to the end of the *cdtC* gene, with the stop

* Corresponding author. Mailing address: Department of Bacteriology, Hiroshima University Graduate School of Biomedical Sciences, Kasumi 1-2-3, Minami-ku, Hiroshima, Hiroshima 734-8553, Japan. Phone: (81) 82 257 5635. Fax: (81) 82 257 5639. E-mail: sugai@hiroshima-u.ac.jp.

codon replaced with a *Bgl*II site (restriction sites are shown in italics). The amplified *cdtABC* gene was ligated into pQE60 in frame at the *Nco*I and *Bgl*II sites, so that the C-terminal CDTC was tagged with six histidine residues. The expression of the *cdtABC* gene was induced by adding isopropyl- β -D-1-thiogalactopyranoside (final concentration of 1 mM; Sigma) at an optical density at 660 nm of 0.5 to 0.7. After induction for 4 h, the culture supernatant was harvested by centrifugation at $5,000 \times g$ for 5 min, and crude proteins were precipitated with ammonium sulfate (final concentration, 80%) by gentle stirring for at least 4 h. The precipitates were recovered by centrifugation at $15,000 \times g$ for 20 min, dissolved in phosphate-buffered saline (PBS) (137 mM NaCl, 2.7 mM KCl, 8.1 mM Na_2HPO_4 , 1.5 mM KH_2PO_4), and dialyzed overnight against PBS. Ni-chelated agarose beads were added into the dialyzed solution and gently shaken for at least 1 h, followed by column chromatography. The column was washed with washing buffer (50 mM NaH_2PO_4 [pH 8.0], 300 mM NaCl, 20 mM imidazole) and eluted with elution buffer (50 mM NaH_2PO_4 [pH 8.0], 300 mM NaCl, 250 mM imidazole). The eluted CDT holotoxin was dialyzed against PBS and concentrated with Centricon 10 concentrators (Millipore, Bedford, Mass.).

Preparation of cells and culture conditions. Peripheral blood mononuclear cells were obtained from healthy volunteers with their informed consent. Twenty to forty milliliters of heparinized venous blood was diluted with an equal volume of PBS with 1% heparin and layered over Ficoll-Hypaque lymphocyte separation medium (ICN Biomedical Inc., Aurora, Ohio). Density gradient centrifugation was performed at $400 \times g$ for 30 min, and mononuclear cells were harvested from the plasma-lymphocyte separation medium interface. Collected cells were washed twice with Earle's balanced salt solution (Nissui, Tokyo, Japan) containing 2.5% fetal calf serum (FCS) (Intergen Co., Purchase, N.Y.). The number of recovered cells was counted and diluted to 10^6 cells/ml in RPMI 1640 containing 10% FCS, 100 U of penicillin G/ml, and 100 μg of streptomycin/ml. The isolated lymphocytes were incubated with CDT (100 ng/ml) and cultured at 37°C in 5% CO_2 , with or without stimulation on day 1 by phytohemagglutinin (PHA) (Difco Lab., Detroit, MI) diluted 1:1,600, and the cell population was monitored for 96 h. A thymic T-cell leukemia cell line, MOLT-4, and a peripheral T-cell leukemia cell line, Jurkat, were maintained in RPMI 1640 containing 10% FCS and 25 μg of kanamycin/ml at 37°C in 5% CO_2 . The cells (10^6 cells/ml) were left untreated or were treated with CDT (100 ng/ml) and cultured under similar conditions. In some experiments, Jurkat cells were similarly treated with 100 ng of anti-CD95 (anti-Fas) monoclonal antibody (Ab) CH11 (BD PharmMingen, San Diego, Calif.) per ml.

Flow cytometry. Conformational changes of the membrane by phosphatidylserine translocation and membrane hole formation were observed by counting the percentages of cells that were stained with fluorescein isothiocyanate (FITC)-labeled annexin V and propidium iodide (PI) in a FACScan flow cytometer (BD Biosciences, San Jose, Calif.). Briefly, CDT-treated cells (5×10^5 to 10×10^5) were collected by centrifugation at $350 \times g$ for 2 min and were washed three times with 500 μl of PBS with 1% FCS. The washed cells were resuspended in 180 μl of PBS with 1% FCS, and 0.5 μl of FITC-labeled annexin V and 1 μl of PI, from the MEBCYTO apoptosis kit (MBL, Nagoya, Japan) were added to the cell suspension. After the reaction for 5 min at room temperature, 10,000 cells were analyzed in the FACScan instrument. The data obtained were processed by quadrant population analysis, using CellQuest software (BD Biosciences). The living cell population was determined by counting cells that were negative for both annexin V and PI (distributed in the lower left of the quadrant).

Caspase assay. CDT-treated cells were harvested and washed with PBS. PBS-washed cells were lysed with lysis buffer (10 mM Tris-Cl [pH 7.4], 25 mM NaCl, 0.25% Triton X-100, 1 mM EDTA) and centrifuged at $15,000 \times g$ for 10 min. The supernatant was diluted with the lysis buffer and the protein concentration was adjusted to 1 mg/ml. Ten micrograms of total protein was incubated in 200 μl of caspase buffer (50 mM Tris-Cl [pH 7.2], 100 mM NaCl, 1 mM EDTA, 10% sucrose, 0.1% CHAPS, and 5 mM dithiothreitol) with a 50 μM concentration (each) of various fluorogenic substrate peptides. The peptides include Ac-DEVD-7-amino-4-methyl coumarine (AMC) for caspase-3, -7, and -8, Ac-DQTD-AMC for caspase-7 and -3, Ac-IETD-AMC for caspase-8, -6, and granzyme, Ac-LEHD-AMC for caspase-9, and Ac-VDVAD-AMC for caspase-2 (Peptide Institute Inc., Osaka, Japan).

The reaction mixture was incubated at 37°C for 60 min, and the release of 7-amino-4-methylcoumarin was measured by use of a spectrophotometer (Shimazu RF-540), with excitation at 380 nm and emission at 460 nm. One unit (U) was defined as 5.2 pmol of substrate cleaved per min per mg of protein.

Various caspase inhibitors were used at a concentration of 100 μM . They were Ac-VAD-fmk as a general caspase inhibitor, Ac-WEHD-CHO for caspase-1, Ac-DEVD-CHO for caspase-3, -7, and -8, Ac-DMQD-CHO for caspase-3, Ac-LEHD-CHO for caspase-9, Ac-IETD-CHO for caspase-8 and -6, Ac-DQTD-

CHO for caspase-7 and -3, and Ac-VDVAD-CHO for caspase-2 (Peptide Institute Inc.).

Electron microscopy. Cells were fixed with 2.5% glutaraldehyde for 2 h and rinsed in 0.1 M cacodylate buffer (pH 7.4) for 12 h. After postfixation with 1% osmium tetroxide for 30 min, cells were stained with 2% uranyl acetate for 30 min and dehydrated in graded alcohol, which was then replaced by propylene oxide. After these steps, the cell suspension was spun down at $8,000 \times g$ for 5 min and the supernatant was discarded. The cell pellets were embedded in epoxy resin. Thin sections were stained in 2% uranyl acetate and lead citrate and were observed in a Hitachi H500 electron microscope.

Preparation of cytosolic and mitochondrial fractions. CDT-treated cells were washed twice with PBS and resuspended in isotonic buffer (10 mM HEPES [pH 7.3], 0.3 M mannitol, 0.1% bovine serum albumin). Digitonin was added to the cell suspension at a concentration of 0.1 mM, and the cells were incubated for 5 min on ice. After the samples were centrifuged at $8,500 \times g$ for 5 min at 4°C, the supernatant was used as the cytosolic fraction. The pellet was resuspended in sonication buffer (50 mM Tris-HCl [pH 7.4], 150 mM NaCl, 2 mM EDTA, 1 mM phenylmethylsulfonyl fluoride, 0.5% Tween 20). The samples were sonicated with an ultrasonic disrupter (UD200 TOMY) for 20 s at output level 4. After centrifugation at $10,000 \times g$ for 5 min at 4°C, the supernatant was collected and used as the mitochondrial fractions.

Antibodies. Antibodies against CDTA, -B, and -C that were previously obtained were used under conditions that were described elsewhere (40). Anti-cytochrome c Ab (BD PharmMingen) was used according to the instructions provided by the supplier.

RESULTS

Cytotoxic effects of highly purified CDT on human peripheral lymphocytes. *A. actinomycetemcomitans* CDT was purified from the culture supernatant of *E. coli* carrying the *A. actinomycetemcomitans cdtABC* genes. The secreted CDT complex was purified through a Ni chelation column, using the affinity of six histidine (His) residues tagged to the C terminus of CDTC (Fig. 1A). Sodium dodecyl sulfate-polyacrylamide gel electrophoresis and immunoblotting detected CDTA', CDTB, and CDTC tagged with six histidine residues in the medium fraction, and premature CDTA was also found in a small amount, suggesting that most of the CDT complex consisted of CDTA', CDTB, and CDTC. Cell distension and the G_2/M blocking activity of purified CDT were confirmed in HeLa cells, and the purified CDT complex was used for experiments.

To address whether CDT can induce cell death of human peripheral lymphocytes, we added purified CDT to peripheral blood mononuclear cell cultures in the presence or absence of PHA stimulation. Flow cytometry analysis with FITC-annexin V and PI revealed that treatment of normal lymphocytes with a combination of CDT and PHA increased the percentage of dead cells (the sum of annexin V⁺ PI⁺ and annexin V⁺ PI⁻ fractions) (Fig. 1B). It should be noted that CDT did not kill lymphocytes very much unless they were activated with PHA. This is in good agreement with the previously suggested activity of CDT, which is cell-cycle-dependent cytotoxicity against HeLa cells (1), and also suggests that CDT can act as an immunosuppressive toxin by killing activated lymphocytes.

CDT induced apoptosis in Jurkat and MOLT-4 cells. In order to obtain further insights into the cytotoxic effect of CDT in T lymphocytes, we used two cell lines, Jurkat and MOLT-4, and monitored population changes in four panels (upper left, upper right, lower left, and lower right [UL, UR, LL, and LR, respectively]) after CDT treatment (Fig. 2). For both cell lines, CDT treatment increased the percentage of dead cells (Fig. 2A). Flow cytometry analysis revealed that the percentage of annexin V⁺ PI⁻ Jurkat cells (distributed in the

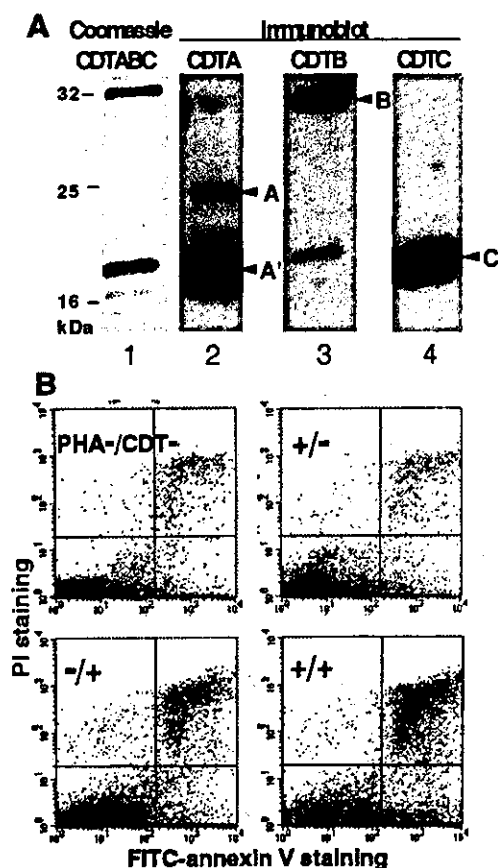


FIG. 1. Cytolethal effect of *A. actinomycetemcomitans* CDT on human peripheral lymphocytes. (A) Purified CDTABC complex in the medium fraction from *E. coli* M15 carrying *A. actinomycetemcomitans* *cdtABC*. Lane 1, Coomassie staining of CDTABC complex; lanes 2 to 4, immunoblots for the detection of each subunit by use of antiserum against CDTA, CDTB, and CDTC, respectively. Arrowheads: A, CDTA (premature form); A', CDTA' (mature form of CDTA); B, mature CDTB; C, mature CDTC tagged with six histidine residues. (B) Flow cytometry analysis. Lymphocytes were stained with FITC-labeled annexin V and PI and analyzed in a FACScan flow cytometer. Lymphocytes prepared from peripheral blood obtained from healthy human volunteers were treated with several combinations of PHA (1:1,600) and CDT (100 ng/ml). A representative result of the quadrant analysis of annexin V- and PI-stained lymphocytes on day 2 is shown.

LR panel) started to increase 8 h after CDT treatment and continued to increase until 24 h after treatment (Fig. 2B). MOLT-4 showed a somewhat different pattern from that of Jurkat. The percentage of annexin V⁺ PI⁻ MOLT-4 cells (LR) started to increase 4 h after CDT treatment and reached a plateau 12 to 16 h after the treatment (Fig. 2B). After that, the annexin V⁺ PI⁻ population (LR) decreased after 16 h. Concomitantly with the increase and decrease of the annexin V⁺ PI⁻ population (LR), the annexin V⁺ PI⁺ population (UR) started to increase after 8 h and kept increasing until 24 h. In both cell lines, the increase of the annexin V⁺ PI⁻ cell population (LR) in the early stage after treatment strongly suggested that CDT poisoning was able to induce apoptosis in cells that are sensitive to Fas-mediated apoptosis as well as in

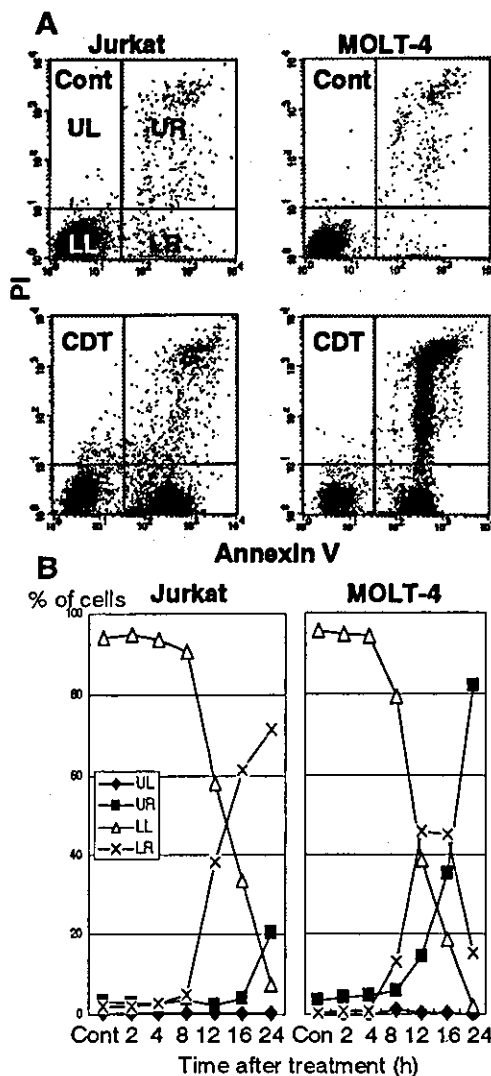


FIG. 2. Cytolethal kinetics on CDT-treated cell lines. T-cell leukemia cell lines Jurkat and MOLT-4 were treated with CDT (100 ng/ml) for various times. Cells stained with FITC-labeled annexin V and PI were analyzed by flow cytometry. (A) Representative results for cells with or without treatment of CDT at 16 h. Cont, control. (B) Kinetics of cell death measured at indicated times after CDT treatment. The percentages of cell populations in the UL quadrant (annexin V⁻ PI⁺, \blacklozenge), the UR quadrant (annexin V⁺ PI⁺, \blacksquare), the LL quadrant (annexin V⁻ PI⁻, \blacktriangle), and the LR quadrant (annexin V⁺ PI⁻, \times) are indicated.

those that are resistant to Fas-mediated apoptosis. We further investigated the apoptotic characteristics of CDT-poisoned cells, including chromosomal DNA fragmentation and chromatin condensation. As shown in Fig. 3A, electrophoretic analysis of the chromosomal DNA of Jurkat cells showed a typical DNA ladder formation after 16 h of treatment with CDT, which is similar to those observed after treatment with anti-Fas Ab or irradiation. Electron microscopic observation of CDT-poisoned Jurkat cells revealed chromatin condensation, which is associated with cells undergoing apoptosis (Fig. 3B). Similar apoptotic characteristics were also apparent for CDT-treated MOLT-4 cells (data not shown). There was no necrotic change,

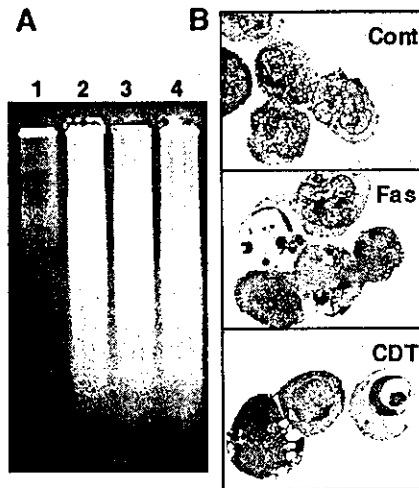


FIG. 3. Apoptotic DNA fragmentation and morphological change in CDT-treated lymphocytes. (A) DNA ladder formation in CDT-treated cells. Jurkat cells were treated with anti-Fas Ab (100 ng/ml) (lane 2), X-ray irradiation (10 Gy) (lane 3), or CDT (100 ng/ml) (lane 4) for 16 h, and chromosomal DNAs were prepared. The extracted DNAs were separated by agarose gel electrophoresis and visualized by staining with ethidium bromide. Lane 1, DNA from untreated Jurkat cells. (B) Ultrastructure of CDT- or anti-Fas Ab-treated lymphocytes. Jurkat cells were treated with CDT (100 ng/ml) for 16 h and subjected to electron microscopic observation as described in Materials and Methods. Cont, control.

such as swelling of the cell body and mitochondria or collapse of the plasma and nuclear membranes, in these cell lines.

Intracellular caspase activities. Apoptosis generally involves the activation of cysteine proteases, or caspases. The activity of sets of the major caspases, caspase-3, -7, and -8, caspase-8 and -6, and caspase-9, in Jurkat and MOLT-4 cells was monitored after CDT treatment. In Jurkat cells, the activity of caspase-3, -7, and -8 started to increase 8 h after treatment of the cells with CDT and significantly increased until 16 to 24 h (Fig. 4). On the other hand, the activity of the caspase-8 and -6 set and caspase-9 slightly increased upon treatment with CDT. Interestingly, caspase activity in MOLT-4 cells started to increase earlier and occurred at a higher level than in Jurkat cells between 4 and 16 h after treatment. After 12 to 16 h, caspase activity in MOLT-4 cells went down in parallel with the appearance of the annexin V⁺ PI⁻ cell population (Fig. 4, Fig. 2B).

Cells retained the phenotype of living cells (annexin V⁻ PI⁻) when the cells were pretreated with a general caspase inhibitor, z-VAD-fmk (100 μ M), indicating that z-VAD-fmk is able to nearly completely inhibit CDT-induced apoptosis (Fig. 5A and B). It also turned out that the CDT-induced elevation of caspase activity could be blocked by z-VAD-fmk (Fig. 5C). These results indicated that CDT-induced apoptotic cell death in Jurkat and MOLT-4 cells was mostly dependent on the activation of a caspase(s) until at least 24 h after treatment.

Signaling pathway of caspases. Caspases can be classified into two categories as follows: initiator caspases, including caspase-2, -8, and -9, which are present upstream of the signaling pathway of apoptosis, and effector caspases, which play

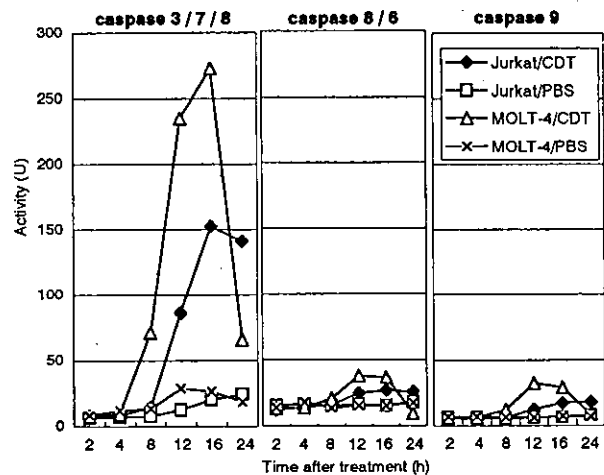


FIG. 4. Caspase activity in CDT-treated lymphocytes. The total protein (10 μ g) was extracted from CDT-treated Jurkat or MOLT-4 cells at the indicated times. Caspase activity was measured by incubation of the extract with a fluorogenic substrate for caspase-3, -7, and -8 (left), caspase-8 and -6 (middle), or caspase-9 (right). After incubation, the released 7-amino-4-methylcoumarin was measured in spectrophotometer, with excitation at 380 nm and emission at 460 nm. \blacklozenge , CDT-treated Jurkat cells; \square , PBS-treated Jurkat cells (control); \triangle , CDT-treated MOLT-4; \times , PBS-treated MOLT-4 (control). The experiments were repeated at least three times, and similar results were obtained. Representative results are shown.

roles in the cleavage of many regulatory proteins (3). In order to determine the signaling pathway of the caspase(s) in CDT-induced apoptosis, we added a variety of caspase inhibitors and monitored their inhibitory effects on CDT cytotoxicity and apoptotic features in Jurkat cells by using flow cytometry with annexin V-PI double staining. For Fas-mediated apoptosis, caspase-8 was confirmed to be a critical initiator caspase for receptor-mediated apoptosis signaling in Jurkat cells, since the addition of Ac-IETD-CHO, an inhibitor of caspase-8 and -6, significantly inhibited the death of Jurkat cells by an anti-Fas Ab (Fig. 6A and C). On the other hand, inhibitors for caspase-3 (Ac-DMQD-CHO), caspase-8 and -6 (Ac-IETD-CHO), and caspase-9 (Ac-LEHD-CHO) failed to inhibit CDT-induced apoptosis of Jurkat cells (Fig. 6B and C), suggesting that CDT-induced apoptosis might use a different signaling pathway from that of Fas-mediated apoptosis. To determine which caspase(s) among those we tested is actually involved in CDT-induced apoptosis, we analyzed the effects of inhibitors of caspase-1 (Ac-WEHD-CHO), caspase-2 (Ac-VDVAD-CHO), and caspase-3, -7, and -8 (Ac-DEVD-CHO) on CDT-induced apoptosis. The inhibitor of caspase-1 (Ac-WEHD-CHO) had no inhibitory effect on CDT-induced apoptosis of Jurkat cells at concentrations up to 200 μ M. On the other hand, CDT-induced apoptosis was dose dependently inhibited by the inhibitor of caspase-2 (VDVAD) or that of caspase-3, -7, and -8 (DEVD) (Fig. 7A and B). However, the combination of inhibitors of caspase-2 (VDVAD) and of caspase-3, -7, and -8 (DEVD) did not show any multiplier effect (Fig. 7C). Together with the fact that inhibitors of caspase-3 (Ac-DMQD-CHO) and caspase-8 and -6 (Ac-IETD-CHO) failed to prevent CDT-induced apoptosis (Fig. 6), our results strongly suggested

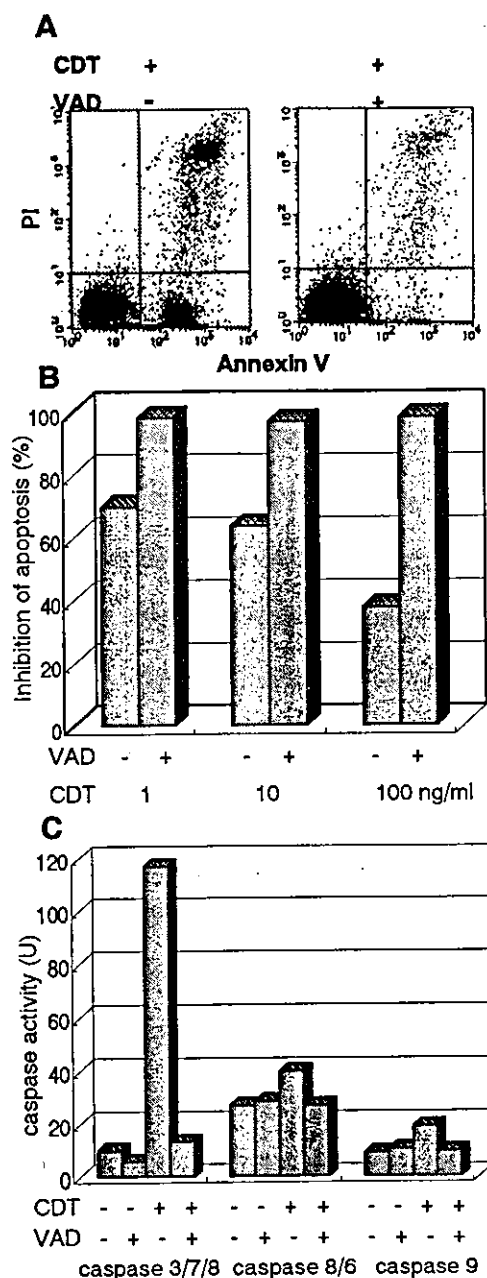


FIG. 5. Effect of general caspase inhibitor on CDT-induced apoptosis. (A) Jurkat cells were preincubated with z-VAD-fmk (100 μ M) for 30 min and then were treated with CDT (1, 10, or 100 ng/ml) for 16 h. Cells were stained with FITC-annexin V and PI and analyzed by flow cytometry. The flow cytometry pattern represents CDT (100 ng/ml)-treated lymphocytes with (+) or without (-) z-VAD-fmk. Inhibition of apoptosis was calculated as the relative percentage of living cells, or the population in the LL quadrant (annexin V⁻ PI⁻ population). (B) z-VAD-fmk inhibits apoptosis in the cells treated with various concentrations of CDT. (C) Effect of z-VAD-fmk on caspase-3, -7, and -8, caspase-8 and -6, and caspase-9 activity induced by CDT. Jurkat cells were preincubated with z-VAD-fmk (100 μ M) for 30 min and then were treated with CDT (100 ng/ml). Caspase activity was measured as described in Materials and Methods.

that caspase-2 and -7 were mainly involved in the activation of this caspase-dependent apoptotic cascade. We therefore measured the activities of caspase-2 and -7 after CDT treatment for 16 h. To measure caspase-7 activity, we used Ac-DQTD-AMC (substrate for caspase-3 and -7) as a substrate because no caspase-7-specific substrate was available. As shown in Fig. 8A, CDT significantly induced the activation of caspase-2. CDT also induced caspase-3 and -7 activity, but the caspase-3-specific inhibitor Ac-DMQD-CHO did not inhibit the activity at all (Fig. 8A). This clearly indicated that the CDT treatment activated caspase-7. These data suggest that caspase-2 and caspase-7 are really involved in the pathway of CDT-induced apoptotic cell death. It is noteworthy that Ac-VDVAD-CHO (caspase-2 inhibitor) showed an inhibitory effect on caspase-3 and -7 activity. Similarly, Ac-DQTD-CHO (the caspase-3 and -7 inhibitor) clearly inhibited the effect on caspase-2. These results suggest that the caspase-2 and -7 pathways of CDT-induced apoptosis are tightly linked to each other, and they are quite consistent with the results of the experiment on the combination effect of inhibitors of caspase-2 and caspase-3, -7, and -8 (Fig. 7C). The incomplete inhibition of caspase-2 activity by Ac-VDVAD-CHO (caspase-2 inhibitor) implies that another molecule with proteolytic activity similar to that of caspase-2 may be involved in CDT-induced cell death.

To determine whether the mitochondrial pathway is really involved in CDT-induced apoptosis, we analyzed the release of cytochrome *c* from mitochondria in CDT-treated cells. As shown in Fig. 8B, the immunoblotting assay revealed that cytochrome *c* was detectable in the cytosol at 8 h, and more apparently so at 16 h, after CDT treatment of Jurkat cells. The appearance of cytochrome *c* accorded well with the time course of caspase activation, suggesting that the mitochondrial pathway is also involved in CDT-induced apoptosis.

DISCUSSION

In order to investigate CDT-induced apoptosis, we first attempted to establish a cell line model of it. Cytological and biological characterizations of CDT-treated Jurkat and MOLT-4 cells satisfied the apoptosis criteria, such as an increase in membrane conformational changes detected by an increase in the annexin V-positive cell population, intranucleosomal DNA fragmentation, chromatin condensation, and an increase in caspase activity (Fig. 1 to 4). It is noteworthy that the elevation of caspase activity in Jurkat and MOLT-4 cells showed some considerable differences in time course and in activation pattern: the culmination of induced caspase activity was higher in CDT-treated MOLT-4 cells than in similarly treated Jurkat cells. This may suggest that Jurkat and MOLT-4 cells took different apoptotic pathways after exposure to CDT. In this context, it should be noted that Jurkat, but not MOLT-4, cells are deficient in p53 (10). p53 is implicated in the G₂/M block in CDT-treated keratinocytes and fibroblasts (7). The phosphorylation of p53 and other phosphorylation signals could play some role in CDT-induced apoptosis, and the lack of p53 might alter the pathway of apoptosis of Jurkat cells from that of MOLT-4 cells.

We tried to obtain further insights into the understanding of the signaling pathway of CDT-induced apoptosis, especially regarding the caspase cascade(s). Caspases are members of the

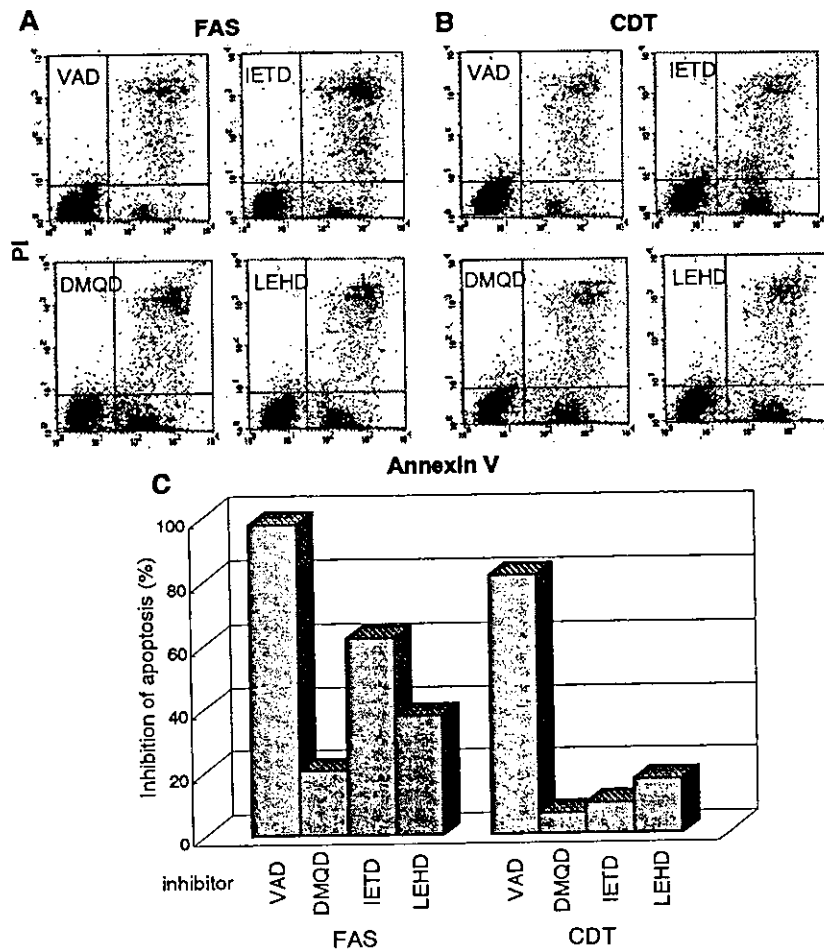


FIG. 6. Effect of various caspase inhibitors on CDT-induced apoptosis. Jurkat cells were preincubated with the indicated inhibitors (100 μ M) for 30 min and then were treated with anti-Fas Ab (100 ng/ml) (A) or CDT (100 ng/ml) (B). After 16 h, cells were stained with FITC-annexin V and PI and analyzed by FACScan. The inhibitors used were VAD (general caspase inhibitor), DMQD (caspase-3 inhibitor), IETD (caspase-8 and -6 inhibitor), and LEHD (caspase-9 inhibitor). (A and B) Representative flow cytometry patterns. (C) Effect of caspase inhibitors on apoptosis induced by anti-Fas Ab (left) or CDT (right). Inhibition of apoptosis was defined as the relative percentage of normal living cells (annexin V⁻ PI⁻).

aspartate-specific cysteine protease family which play a critical role in apoptosis (6, 39). They are composed of two major subfamilies, initiator caspases and effector caspases, based on the presence or absence of a large prodomain in the amino-terminal region (33). Initiator caspases generally act upstream of the proteolytic cascade, while effector caspases act downstream and are involved in the cleavage of specific cellular substrate proteins (41). Once processed, the substrates induce morphological changes characteristic of the apoptotic process (8, 11). The long prodomains of the initiator caspases trigger and/or facilitate the activation of proenzymes through interactions with adaptor molecules (13). Caspase-2, -8, -9, and -10 generally act as initiator caspases upstream of the cascade of effector caspases with small prodomains, such as caspase-3, -6, and -7 (26). Among the caspases, caspase-8, -9, and -10 play a fundamental role in transducing the specific apoptotic signal, and they cleave and activate effector procaspase-3, -6, and -7 (4). Effector caspases, in turn, cleave various proteins, leading to morphological and biochemical features characteristic of

apoptosis. Recently, it has become clear that caspase-9 is involved in the apoptotic pathway that relies on mitochondrial dysfunction (15). Caspase-8 and -10 are involved in the apoptosis pathway mediated by death receptors (2).

Our results indicated that inhibitors of caspase-2 and -7 showed inhibitory effects on CDT-induced apoptosis. Several bacterial toxins are known to induce apoptosis through caspase-dependent pathways, although the exact molecular mechanism of the signaling cascade has not been well characterized. For instance, Shiga toxin and Shiga-like toxin have been demonstrated to activate caspase-2, -3, -6, -8, and -9 (5, 17, 18). It was suggested that these toxins use the caspase cascade involved in Fas-mediated apoptosis. Other toxins, such as *E. coli* heat-labile enterotoxin (32), *Clostridium difficile* toxin B (29), diphtheria toxin (19), and *Mannheimia haemolytica* leukotoxin (23), were shown to induce caspase-3. However, a detailed caspase cascade induced by bacterial toxins has not been well established. To our knowledge, this is the first report that a bacterial toxin preferentially utilizes caspase-2 and -7 in

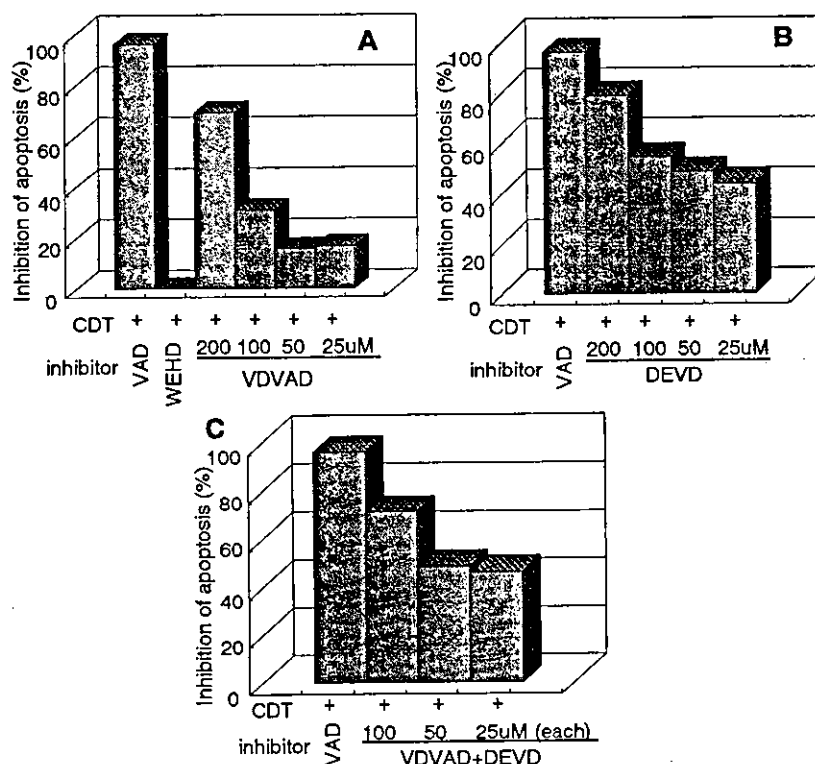


FIG. 7. Dose-dependent inhibitory effects of caspase inhibitors on CDT-induced apoptosis. Jurkat cells were preincubated with various concentrations of caspase inhibitors (25, 50, 100, and 200 μ M) for 30 min and then were treated with CDT (100 ng/ml). The inhibitors used were WEHD (caspase-1 inhibitor), VDVAD (caspase-2 inhibitor), and DEVD (caspase-3, -7, and -8 inhibitor). After 16 h, cells were stained with FITC-annexin V and PI and analyzed by flow cytometry. Panels show the relative inhibition of CDT-induced apoptosis with VDVAD (A), DEVD (B), and VDVAD and DEVD (C). Inhibition of apoptosis was defined as the relative percentage of living cells (annexin V⁻ PI⁻). VAD (general caspase inhibitor) and WEHD were used at concentrations of 100 and 200 μ M, respectively.

the signaling pathway for apoptosis. In recent studies, caspase-2 was implicated in the release of cytochrome *c* from mitochondria in stress-induced apoptotic pathways (16, 22, 27, 30). One such stress-inducing agent is a topoisomerase II poison, etoposide, that induces double-stranded DNA breaks in cells. Robertson et al. (30) demonstrated that etoposide-induced DNA damage induces activation of caspase-2 and hence results in cytochrome *c* release from mitochondria and subsequent apoptosis. It is interesting that a possible mechanism by which CDT can induce cytopathic effects involves DNA strand breaks induced by its putative DNase activity (12, 20). Such CDT-induced DNA damage may trigger the mitochondrial cascade including caspase-2 and -7. A recent report has indicated the requirement of caspase-2 for the initiation of stress-induced apoptosis prior to mitochondrial permeabilization (22). In our case, CDT-induced DNA damage may directly activate caspase-2 and then induce the mitochondrial cascade, probably followed by caspase-7 activation. Caspase-7 is a late signal transducer and one of the members of the apoptosome complex which is activated by mitochondrial stress (3). Both caspase-2 and -7 are involved in stress-induced cascades, suggesting that CDT-induced apoptosis is related to the mitochondrial pathway. Our present results indicate that CDT can induce mitochondrial membrane permeabilization, resulting in the release of cytochrome *c*, and that this mitochondrial path-

way is highly involved in CDT-induced apoptosis. This is quite in agreement with an experiment showing that Bcl-2 overexpression reduces apoptosis in a CDT-treated human B lymphoblastoid cell line, JY (35).

Fas ligation on the cell surface induces apoptosis through the receptor-mediated signaling pathway, which involves caspase-8 as an initiation signal (2). The fact that caspase-8 inhibitor blocked Fas-mediated apoptosis in Jurkat cells (Fig. 6) indicated that the Fas-dependent apoptotic pathway was active in this cell line. In contrast, no inhibitory effect of caspase-8 inhibitor on CDT-induced apoptosis was observed in Jurkat cells, suggesting that the cytotoxic effect of CDT does not require the activation of death receptors on the cell surface.

Since CDT is able to induce apoptosis of activated T cells, this toxin may play an important role in that the bacteria evade T-cell immune responses in the periodontal pocket. It is conceivable that CDT produced by this pathogen exacerbates local inflammation by inducing apoptotic cell death of T lymphocytes that are responsible for the clearance of bacteria from the periodontal pocket. Further studies on the effect of CDT on the caspase network should unveil the CDT-related signal transduction pathway in T-lymphocyte apoptosis that may lead to the suppression of immune responses to the pathogen.

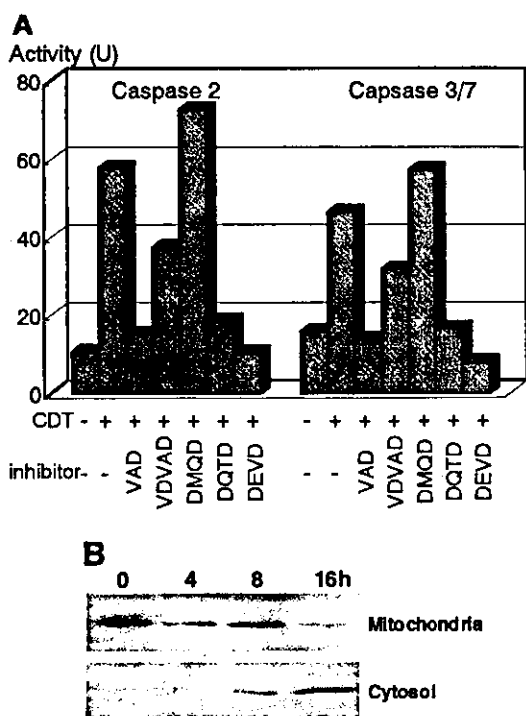


FIG. 8. Elevation of caspase-2 or -7 activity and cytochrome *c* release by CDT treatment. (A) Jurkat cells were preincubated with the indicated inhibitor (100 μ M) for 30 min and then were treated with CDT (100 ng/ml) for 16 h. The inhibitors used were VAD (general caspase inhibitor), VDVAD (caspase-2 inhibitor), DMQD (caspase-3 inhibitor), DQTD (caspase-3 and -7 inhibitor), and DEVD (caspase-3, -7, and -8 inhibitor). Caspase activity was measured as described in Materials and Methods. (B) Cytosol and mitochondrial fractions were extracted from Jurkat cells that were treated with CDT (100 ng/ml) for 0, 4, 8, and 16 h and were subsequently immunoblotted with an anti-cytochrome *c* Ab followed by a horseradish peroxidase-conjugated secondary Ab. The bands of cytochrome *c* were visualized by ECL.

ACKNOWLEDGMENTS

We thank Kei Nakachi, Donald G. MacPhee, and Seishi Kyoizumi at the Department of Radiobiology and Molecular Epidemiology, Radiation Effects Research Foundation, for helpful suggestions. We thank the Research Facilities, Hiroshima University School of Dentistry and School of Medicine, for the use of facilities.

This study was supported in part by a Grant for Development of Highly Advanced Medical Technology (A) and by a Grant-in-Aid for Scientific Research (B) from the Ministry of Education, Science, Sports and Culture of Japan.

REFERENCES

- Alby, F., R. Mazars, J. De Rycke, E. Guillou, V. Baldin, J.-M. Darbon, and B. Ducommun. 2001. Study of the cytolethal distending toxin (CDT)-activated cell cycle checkpoint. Involvement of the CHK2 kinase. *FEBS Lett.* 491:261-265.
- Ashkenazi, A., and V. M. Dixit. 1998. Death receptors: signaling and modulation. *Science* 281:1305-1308.
- Bratton, S. B., M. Macfarlane, K. Cain, and G. M. Cohen. 2000. Protein complexes activate distinct caspase cascades in death receptor and stress induced apoptosis. *Exp. Cell Res.* 256:27-33.
- Budihardjo, I., H. Oliver, M. Lutter, X. Luo, and X. Wang. 1999. Biochemical pathways of caspase activation during apoptosis. *Annu. Rev. Cell Dev. Biol.* 15:269-290.
- Ching, J. C., N. L. Jones, P. J. Ceponis, M. A. Karmali, and P. M. Sherman. 2002. *Escherichia coli* Shiga-like toxins induce apoptosis and cleavage of poly(ADP-ribose) polymerase via in vitro activation of caspases. *Infect. Immun.* 70:4669-4677.
- Cohen, G. M. 1997. Caspases: the executioners of apoptosis. *Biochem. J.* 326:1-16.
- Cortes-Bratti, X., C. Karlsson, T. Lagergard, M. Thelestam, and T. Frisan. 2001. The *Haemophilus ducreyi* cytolethal distending toxin induces cell cycle arrest and apoptosis via the DNA damage checkpoint pathways. *J. Biol. Chem.* 276:5296-5302.
- Cryns, V., and J. Yuan. 1998. Proteases to die for. *Genes Dev.* 12:1551-1570.
- Deng, K., J. L. Latimer, D. A. Lewis, and E. J. Hansen. 2001. Investigation of the interaction among the components of the cytolethal distending toxin of *Haemophilus ducreyi*. *Biochem. Biophys. Res. Commun.* 20:609-615.
- Dreyfus, D. H., M. Nagasawa, C. A. Kelleher, and E. W. Gelfand. 2000. Stable expression of Epstein-Barr virus BZLF-1-encoded ZEBRA protein activates p53-dependent transcription in human Jurkat T-lymphoblastoid cells. *Blood* 96:625-634.
- Earnshaw, W. C., L. M. Martins, and S. H. Kaufmann. 1999. Mammalian caspases: structure, activation, substrates, and functions during apoptosis. *Annu. Rev. Biochem.* 68:383-424.
- Etwell, C. A., K. Chao, K. Patel, and L. A. Dreyfus. 2001. *Escherichia coli* CdtB mediates cytolethal distending toxin cell cycle arrest. *Infect. Immun.* 69:3418-3422.
- Fesik, S. W. 2000. Insights into programmed cell death through structural biology. *Cell* 103:273-282.
- Frisk, A., M. Labens, C. Johansson, H. Ahmed, L. Svensson, K. Ahlman, and T. Lagergard. 2001. The role of different protein components from the *Haemophilus ducreyi* cytolethal distending toxin in the generation of cell toxicity. *Microb. Pathog.* 30:313-324.
- Green, D. R. 2000. Apoptotic pathways: paper wraps stone blunts scissors. *Cell* 102:1-4.
- Guo, Y., S. M. Srinivasula, A. Druilhe, T. Fernandes-Alnemri, and E. S. Alnemri. 2002. Caspase-2 induces apoptosis by releasing proapoptotic proteins from mitochondria. *J. Biol. Chem.* 277:13430-13437.
- Kiyokawa, N., T. Mori, T. Taguchi, M. Saito, K. Mimori, T. Suzuki, T. Sekino, N. Sato, H. Nakajima, Y. U. Katagiri, T. Takeda, and J. Fujimoto. 2001. Activation of the caspase cascade during Stx-1-induced apoptosis in Burkitt's lymphoma cells. *J. Cell. Biochem.* 81:128-142.
- Kojio, S., H. Zhang, M. Ohmura, F. Gondaira, N. Kobayashi, and T. Yamamoto. 2000. Caspase-3 activation and apoptosis induction coupled with the retrograde transport of Shiga toxin: inhibition by brefeldin A. *FEMS Immunol. Med. Microbiol.* 29:275-281.
- Komatsu, N., T. Oda, and T. Muramatsu. 1998. Involvement of both caspase-like proteases and serine proteases in apoptotic cell death induced by ricin, modeccin, diphtheria toxin, and pseudomonas toxin. *J. Biochem. (Tokyo)* 124:1038-1044.
- Lara-Tejero, M., and J. E. Galan. 2000. A bacterial toxin that controls cell cycle progression as a deoxyribonuclease I-like protein. *Science* 290:354-357.
- Lara-Tejero, M., and J. E. Galan. 2001. CdtA, CdtB, and CdtC form a tripartite complex that is required for cytolethal distending toxin activity. *Infect. Immun.* 69:4358-4365.
- Lassus, P., X. Opitz-Araya, and Y. Lazebnik. 2002. Requirement for caspase-2 in stress-induced apoptosis before mitochondrial permeabilization. *Science* 297:1352-1354.
- Leite, F., S. O'Brien, M. J. Sylte, T. Page, D. Atapattu, and C. J. Czuprynski. 2002. Inflammatory cytokines enhance the interaction of *Mannheimia haemolytica* leukotoxin with bovine peripheral blood neutrophils in vitro. *Infect. Immun.* 70:4336-4343.
- Lewis, D. A., M. K. Stevens, J. L. Latimer, C. K. Ward, K. Deng, R. Blick, S. R. Lumley, C. A. Ison, and E. J. Hansen. 2001. Characterization of *Haemophilus ducreyi* *cdtA*, *cdtB*, and *cdtC* mutants in vitro and in vivo systems. *Infect. Immun.* 69:5626-5634.
- Mangan, D. F., N. S. Taichman, E. T. Lally, and S. M. Wahl. 1991. Lethal effects of *Actinobacillus actinomycetemcomitans* leukotoxin on human T lymphocytes. *Infect. Immun.* 59:3267-3272.
- Nicholson, D. W., and N. A. Thornberry. 1997. Caspases: killer proteases. *Trends Biochem. Sci.* 22:299-306.
- Paroni, G., C. Henderson, C. Schneider, and C. Brancolini. 2002. Caspase-2 can trigger cytochrome *c* release and apoptosis from the nucleus. *J. Biol. Chem.* 277:15147-15161.
- Pickett, C. L., and C. A. Whitehouse. 1999. The cytolethal distending toxin family. *Trends Microbiol.* 7:292-297.
- Qa'Dan, M., M. Ramsey, J. Daniel, L. M. Spyras, B. Safiejko-Mroccka, W. Ortiz-Leduc, and J. D. Ballard. 2002. *Clostridium difficile* toxin B activates dual caspase-dependent and caspase-independent apoptosis in intoxicated cells. *Cell. Microbiol.* 4:425-434.
- Robertson, J. D., M. Enoksson, M. Suomela, B. Zhivotovsky, and S. Orrenius. 2002. Caspase-2 acts upstream of mitochondria to promote cytochrome *c* release during etoposide-induced apoptosis. *J. Biol. Chem.* 277:29803-29809.
- Saiki, K., K. Konishi, T. Gomi, T. Nishihara, and M. Yoshikawa. 2001. Reconstitution and purification of cytolethal distending toxin of *Actinobacillus actinomycetemcomitans*. *Microbiol. Immunol.* 45:497-506.
- Salmond, R. J., R. S. Pitman, E. Jimi, M. Soriani, T. R. Hirst, S. Ghosh, M. Rincon, and N. A. Williams. 2002. CD8⁺ T cell apoptosis induced by *Esch-*

- erichia coli* heat-labile enterotoxin B subunit occurs via a novel pathway involving NF-kappaB-dependent caspase activation. *Eur. J. Immunol.* **32**: 1737-1747.
33. Salvesen, G. S., and V. M. Dixit. 1999. Caspase activation: the induced-proximity model. *Proc. Natl. Acad. Sci. USA* **96**:10964-10967.
34. Shenker, B. J., R. H. Hoffmaster, T. L. McKay, and D. R. Demuth. 2000. Expression of the cytolethal distending toxin (Cdt) operon in *Actinobacillus actinomycescomitans*: evidence that the CdtB protein is responsible for G₂ arrest of the cell cycle in human T cells. *J. Immunol.* **165**:2612-2618.
35. Shenker, B. J., R. H. Hoffmaster, A. Zekavat, N. Yamaguchi, E. T. Lally, and D. Demuth. 2001. Induction of apoptosis in human T cells by *Actinobacillus actinomycescomitans* cytolethal distending toxin is a consequence of G₂ arrest of the cell cycle. *J. Immunol.* **167**:435-441.
36. Shenker, B. J., T. McKay, S. Datar, M. Miller, R. Chowhan, and D. Demuth. 1999. *Actinobacillus actinomycescomitans* immunosuppressive protein is a member of the family of cytolethal distending toxins capable of causing a G₂ arrest in human T cells. *J. Immunol.* **162**:4773-4780.
37. Shenker, B. J., L. Vitale, and C. King. 1995. Induction of human T cells that coexpress CD4 and CD8 by an immunomodulatory protein produced by *Actinobacillus actinomycescomitans*. *Cell. Immunol.* **164**:36-46.
38. Slots, J., H. S. Reynolds, and R. J. Genco. 1980. *Actinobacillus actinomycescomitans* in human periodontal disease: a cross-sectional microbiological investigation. *Infect. Immun.* **29**:1013-1020.
39. Stennicke, H. R., and G. S. Salvesen. 1997. Biochemical characteristics of caspases-3, -6, -7, and -8. *J. Biol. Chem.* **272**:25719-25723.
40. Sugai, M., T. Kawamoto, S. Y. Peres, Y. Ueno, H. Komatsuzawa, T. Fujiwara, H. Kurihara, H. Suginaka, and E. Oswald. 1998. The cell cycle-specific growth-inhibitory factor produced by *Actinobacillus actinomycescomitans* is a cytolethal distending toxin. *Infect. Immun.* **66**:5008-5019.
41. Thornberry, N. A., and Y. Lazebnik. 1998. Caspases: enemies within. *Science* **281**:1312-1316.

Editor: V. J. DiRita

Expression Characteristics and Stimulatory Functions of CD43 in Human CD4⁺ Memory T Cells: Analysis Using a Monoclonal Antibody to CD43 That Has a Novel Lineage Specificity¹

Seishi Kyoizumi,^{2*} Takaaki Ohara,[†] Yoichiro Kusunoki,^{*} Tomonori Hayashi,^{*} Kazuaki Koyama,^{*} and Naohiro Tsuyama[‡]

We have used HSCA-2, an mAb that recognizes a sialic acid-dependent epitope on the low molecular mass (~115-kDa) glycoform of CD43 that is expressed in resting T and NK cells, to examine the expression characteristics and stimulatory functions of CD43 in human CD4⁺ memory T cells. Having previously reported that the memory cells that respond to recall Ags in a CD4⁺CD45RO⁺ T cell population almost all belong to a subset whose surface CD43 expression levels are elevated, we now find that exposing these same memory T cells to HSCA-2 mAb markedly increases their proliferative responsiveness to recall Ags. We think it unlikely that this increase in responsiveness is a result of CD43-mediated monocyte activation, especially given that the HSCA-2 mAb differs from all previously used CD43 mAbs in having no obvious binding specificity for monocyte CD43. Predictably, treatment with HSCA-2 mAb did not lead to significant recall responses in CD4⁺CD45RO⁺ T cells, whose CD43 expression levels were similar to or lower than those of naive cells. Other experiments indicated that the HSCA-2 mAb was capable of enhancing the proliferative responsiveness of CD4⁺ memory T cells that had been exposed to polyclonal stimulation by monocyte-bound CD3 mAb and could also act in synergy with CD28 mAb to enhance the responsiveness of CD4⁺ T cells to CD3 stimulation. Taken together, these findings suggest that the CD43 molecules expressed on CD4⁺ memory T cells may be capable of enhancing the costimulatory signaling and hence providing accessory functions to TCR-mediated activation processes. *The Journal of Immunology*, 2004, 172: 7246–7253.

CD43 (leukosialin) is a highly glycosylated transmembrane protein that is expressed in all hemopoietic cells except resting mature B cells and erythrocytes (1, 2). All CD43 molecules possess extracellular domains that consist of multiple *O*-linked carbohydrate chains (3) and show considerable m.w. heterogeneity due to differential glycosylation (4). Even within T cell populations there are at least two glycoforms of CD43 that are recognized by different mAbs. The lighter of these glycoforms has a molecular mass of 95–115 kDa, whereas that of that heavier one is between 130 and 135 kDa (5, 6). Interestingly, the heavier glycoform contains core 2 *O*-glycans, appears to be up-regulated during T cell activation (5, 7), and can be used to distinguish between memory and effector CD8⁺ T cells in mice (8, 9). It is not yet clear exactly what CD43 does in T cells, however, especially in view of

the continued existence of a number of unresolved controversies about its roles in such key processes as cell adhesion, cell death, and costimulation in TCR signaling (10).

It has, for instance, been claimed that CD43 molecules may have antiadhesive as well as proadhesive functions in T cell trafficking (9, 11–14). It has also been claimed that up-regulation of CD43 expression can have a negative effect on activation-induced cell death of T cells (15), and that Ab-mediated cross-linking of CD43 induces apoptosis of Jurkat T cells (16). CD43 also appears to play a role in T cell activation, but precisely what role remains unclear. There are, for example, Ab cross-linking experiments involving CD43 that suggest that it may have a costimulatory role in vitro (17) and act in association with the phosphorylation of signal-transducing molecules in T cell activation (18–20); other experiments using CD43-deficient mice suggest, on the contrary, that CD43 has either a negative regulatory role as a steric barrier (21) or possibly even no significant role at all (22) in T cell activation. There are several recent reports suggesting that molecular complexes between CD43 and cytoskeletal adaptor proteins are probably excluded from the immunological synapse in T cell activation in vitro (23–25) and in vivo (26). Some of these reports include suggestions that this relocalization of CD43 is necessary for activation-induced cytokine production (23, 27), although there is at least one recent study that comes to precisely the opposite conclusion (28). The functional significance of redistribution of CD43 in T cell activation is therefore very unclear. Nevertheless, given that CD43 expression levels appear to be considerably elevated in memory T cell populations in humans (29–31) and mice (15), it seems reasonable to assume that CD43 has an important part to play in one or more aspects of the memory T cell responses.

*Laboratory of Immunology, Department of Radiobiology/Molecular Epidemiology, Radiation Effects Research Foundation, Hiroshima, Japan; †Life Science Laboratories, Life Science RD Center, Kaneka Corp., Takasago, Japan; and ‡Cellular Signal Analysis, Department of Bio-Signal Analysis, Applied Medical Engineering Science, Yamaguchi University Graduate School of Medicine, Ube City, Japan

Received for publication November 11, 2003. Accepted for publication April 2, 2004.

The costs of publication of this article were defrayed in part by the payment of page charges. This article must therefore be hereby marked *advertisement* in accordance with 18 U.S.C. Section 1734 solely to indicate this fact.

¹ This publication is based on research performed at the Radiation Effects Research Foundation (RERF), Hiroshima and Nagasaki, Japan. RERF is a private nonprofit foundation funded equally by the Japanese Ministry of Health, Labor, and Welfare (MHLW) and the U.S. Department of Energy, the latter through the National Academy of Sciences. This work was supported by RERF Research Protocols 1-93 and 4-02 and in part by funds for Research Promotion on AIDS Control from MHLW.

² Address correspondence and reprint requests to Dr. Seishi Kyoizumi, Laboratory of Immunology, Department of Radiobiology/Molecular Epidemiology, Radiation Effects Research Foundation, 5-2 Hijiyama Park, Minami Ward, Hiroshima 732-0815, Japan. E-mail address: kyoizumi@rerf.or.jp

We have recently described how HSCA-2, a novel CD43 mAb, can be used for the classification of human CD4⁺CD45RO⁺ memory T cells into three subsets on the basis of differences in their CD43 expression (31). In this classification, cells of the first of the three subsets (the M1 subset) express elevated levels of CD43, whereas cells of the M2 subset express CD43 levels similar to those of naive cells, and cells of the M3 subset express reduced CD43 levels. We also found that the M1 subset contains the highest proportion of recall Ag-reactive precursors and secretes substantially more IFN- γ and IL-4. The majority of effector memory T cells (CCR7⁻) (32) are assumed to belong to this subset (31). However, as ~70% of the cells in the M1 subset express CCR7, the subset may also contain central memory T cells. The M2 subset cells are less mature memory cells that retain longer telomeres than do cells of the M1 and M3 subsets, and their memory functionality (including recall Ag reactivity) appears to be marginal (31). The M3 subset consists of cells that are anergic to TCR-mediated stimuli and prone to apoptosis (31). As the level of CD43 expression is correlated with recall Ag reactivity, it is possible that CD43 molecules will prove to have some accessory role in the activation of human CD4⁺ memory T cells.

In this paper we describe immunological properties and expression characteristics of the CD43 molecules that are recognized by HSCA-2 mAb. We go on to examine the functional properties of these molecules in the proliferative responses of CD4⁺ memory T cells. The results described in this report demonstrate that the HSCA-2 mAb specifically recognizes a neuraminidase-sensitive epitope of a low molecular mass glycoform (115 kDa) of CD43 that is predominantly expressed in lymphoid populations. It is also suggested that the CD43 glycoform recognized by HSCA-2 mAbs could play an accessory part in the recall Ag-specific responses of mature CD4⁺ memory T cells (i.e., M1 subset cells). HSCA-2 mAb has therefore proven to be a useful molecular probe for both the classification and the functional analysis of human CD4⁺ memory T cells. The implications of our work for the involvement of CD43-mediated stimulatory signaling in the activation of CD4⁺ T cells are discussed.

Materials and Methods

Production of HSCA-2 mAb

The HSCA-2 hybridoma is a product of the fusion of NS1 mouse myeloma cells with splenocytes from BALB/c mice immunized by injection of human KG-1 cells (31). Immunization, fusion, selection, and cloning protocols were essentially as described previously (33). Hybridoma supernatants were initially screened for reactivity with KG-1 cells by indirect immunofluorescence. The HSCA-2 hybridoma was selected for further study because of its unique specificity of reactivity with PBMC and cord blood CD34⁺ stem cells. Isotype characterization showed that the HSCA-2 mAb was of the IgG1 subclass. Ascites fluid was obtained from SCID mice injected with the HSCA-2 hybridoma. After purification from ascites fluid by DE52 ion exchange chromatography, HSCA-2 mAb was labeled with FITC (Sigma-Aldrich, St. Louis, MO) for flow cytometry. Fab of HSCA-2 mAb were prepared by digestion with papain (34). This mAb was filed for participation in the Eighth International Workshop and Conference on Human Leukocyte Differentiation Antigens (to be held in Adelaide, Australia).

Other mAbs

Unconjugated CD28 mAb (clone CD28.2) (35), used for T cell culture, was purchased from Coulter-Immunotech (Marseilles, France). Unconjugated and FITC-conjugated CD43 mAbs, DFT-1 (1), L10 (36), and IG10 (37), were obtained from Coulter-Immunotech, Caltag Laboratories (Burlingame, CA), and BD Pharmingen (San Diego, CA), respectively. PE-labeled CD4, CD8, CD14, CD19, and CD56 mAbs and PerCP-labeled CD4 and CD8 mAbs were purchased from BD Biosciences (San Jose, CA). PE-labeled CD45RO mAb was obtained from Caltag Laboratories.

Transfection of CD43 cDNA

Total RNA of KG-1 cells was isolated with TRIzol reagent (Invitrogen, Carlsbad, CA). First-strand cDNA primed with oligo(dT)₃₀ was synthesized using SuperScript II reverse transcriptase (Invitrogen). CD43 cDNA was PCR-amplified with the primers 5'-ctctgtcctcctgctgtttgc-3' and 5'-catgggtgggtgctgttaa-3' using Advantage cDNA polymerase mix (Clontech Laboratories, Palo Alto, CA) and cloned into pCR2.1 TA cloning vector (Invitrogen). The sequence-verified clone was recloned into the *EcoRI* site of pIRESneo (Clontech Laboratories) and designated pIRESneo hCD43. Subsequently, 30 μ g of pIRESneo hCD43 or pIRESneo (negative control) was electroporated into 2×10^6 HeLa cells in 200 μ l of PBS by GenePulser (Bio-Rad, Hercules, CA) at 0.7 kV and 25 μ F. Cells were treated with 1 mg/ml G418 for 2 wk. Drug-resistant colonies were selected and expanded to confirm CD43 expression by flow cytometry. HeLa transfectant cells expressing high levels of CD43 were isolated by a cell sorter for additional experiments.

Cell preparations and flow cytometry

For direct immunofluorescence of cultured cell lines, 2×10^5 CD43- or mock-transfected HeLa and KG-1 cells were stained with 1 μ g of FITC-labeled HSCA-2, DFT-1, and MOPC21 mAbs for 45 min on ice. For the analyses of CD43 glycoepitopes, 2×10^6 KG-1 cells were treated with neuraminidase (0.1 U/ml in PBS) for 30 min at 37°C. For competitive inhibition, KG-1 cells were pretreated with various amounts of HSCA-2 or DFT-1 mAbs (12.5–200 μ g/ml) for 1 h on ice and then stained with FITC-labeled HSCA-2 and DFT-1 mAbs for 45 min. FACSscan (BD Biosciences) was used for flow cytometric analyses.

For flow cytometry of human blood cells, PBMCs from healthy adult volunteers ($n = 6$) and cord blood mononuclear cells ($n = 3$) were isolated by density centrifugation in Ficoll-Hypaque (density, 1.077 g/ml; ICN Bio-medical, Aurora, OH). Granulocytes were isolated by double-layered density centrifugation in Ficoll-Hypaque (density, 1.077 and 1.119 g/ml; Wako Pure Chemical, Osaka, Japan) according to the manufacturer's instructions. For isolation of monocytes, CD14⁺ cells were purified from PBMCs by positive enrichment using autoMACS (Miltenyi Biotec, Bergish Gladbach, Germany) according to the manufacturer's instructions. Enriched monocytes also were used for immunoprecipitation and proliferation assay, as described below.

For single-color analysis of purified monocytes and granulocytes, cells were stained with FITC-labeled CD43 mAbs and analyzed by flow cytometry with a gate in a region for monocytes or granulocyte fractions on the forward and side light scatter profiles. For two-color analysis of lymphocytes, PBMCs were stained with PE-labeled CD4, CD8, CD19, and CD56 in combination with FITC-labeled CD43 mAbs. Cord blood mononuclear cells were stained with FITC-labeled CD43 and PE-labeled CD34 mAbs. For triple-color analysis, PBMCs were stained with FITC-labeled CD43, PE-conjugated CD45RO, and PerCP-labeled CD4 mAbs. CD4⁺ lymphocytes were gated on forward/side scatter and PerCP fluorescence. The proportions of CD4⁺ CD45RO⁻ cells (RO⁻ subset) and CD4⁺ CD45RO⁺ cells expressing high (M1 subset), intermediate (M2), and low (M3) levels of CD43 were measured by flow cytometry with FACSscan (see Fig. 4).

For preparation of activated CD4⁺ T cells, MACS-purified CD4⁺ T cells were stimulated with immobilized anti-CD3 mAb (OKT-3) in the presence of IL-2 (10 ng/ml) for 4 days in RPMI 1640 supplemented with 10% FCS. Immobilized CD3 mAb was prepared by binding OKT3 mAb (10 μ g/ml in sodium bicarbonate buffer, pH 9.6) in 24-well plates at room temperature for 2 h, then washing the plates with RPMI 1640 supplemented with 10% FCS.

For isolation of the four CD4⁺ T cell subsets, M1, M2, M3, and CD45RO⁻, CD4⁺ cells were purified by negative enrichment using MACS as described previously (31). MACS-purified CD4⁺ T cells were stained with FITC-labeled HSCA-2 and PE-labeled CD45RO mAbs. After incubation with propidium iodide at 10 μ g/ml for 15 min to gate out dead cells, CD4⁺ T cells in the four subsets were sorted by a single laser cell sorter (FACSstar; BD Biosciences). During cell sorting, stained and sorted cell suspensions were maintained at 4°C by a cooling circulation system.

Cell proliferation assay

For proliferative response to recall Ags, PBMCs (5×10^4 cells/well) in 96-well, flat-bottom plastic plates were stimulated with tuberculosis purified protein derivative (PPD;³ Connaught Laboratories, Ontario, Canada) or tetanus toxoid (TT; Calbiochem, La Jolla, CA) at 5 μ g/ml. For total and subset CD4⁺ T cells, T cells (5×10^4 cells/well) were stimulated with

³ Abbreviations used in this paper: PPD, purified protein derivative; TT, tetanus toxoid.

these recall Ags in the presence of autologous monocytes (2.5×10^4 cells/well) that were previously isolated using autoMACS with anti-CD14 Ab (Miltenyi Biotec) and irradiated with x-ray at 30 Gy. The culture medium used for this assay was RPMI 1640 supplemented with 10% human serum. For proliferative responses to anti-CD3 mAb, total CD4⁺ T cells or sorted subset T cells were stimulated with various concentrations of soluble CD3 (OKT-3) mAb (0.0001–1 μ g/ml) in the presence of autologous monocytes. The culture medium used for this assay was RPMI 1640 medium supplemented with 10% FCS.

The effects of CD43 (0.05–5 μ g/ml) and CD28 mAbs (1 μ g/ml) on cell proliferation were evaluated. Proliferation was measured on day 3 for CD3 mAb and on day 5 for PPD by adding [³H]thymidine (NEN, Boston, MA) at 1 μ Ci/well during the last 16 h of culture. All cultures were set up in triplicate.

Immunoprecipitation

Cells used for immunoprecipitation were KG-1 cells, PBMCs, MACS-purified CD14⁺ monocytes, PBMCs depleted with CD14⁺ monocytes, MACS-purified CD4⁺ T cells, and activated CD4⁺ T cells. Cells (5×10^6 – 1×10^7) were labeled at the cell surface by lactoperoxidase-catalyzed iodination as described previously (38). Radioiodinated cells were lysed with extraction buffer (0.5% Nonidet P-40, 10 mM Tris-HCl, 0.15 M NaCl, 1 mM PMSF, and 0.02% NaN₃) for 10 min on ice. The mixture was centrifuged at $27,000 \times g$ at 4°C for 20 min, and the supernatant was collected. Immunoprecipitations were performed by incubating radio-

labeled cell lysate with 10 μ g of HSCA-2, DFT-1, or MOPC21 mAbs for 1 h on ice, then adding a 20 μ l-packed volume of protein G-Sepharose (Amersham Pharmacia Biotech, Piscataway, NJ), and further incubating the mixture for 30 min. Immunoprecipitates were washed four times in extraction buffer and solubilized in reducing Laemmli sample buffer subjected to SDS-PAGE (7.5% gel). After fixing and drying, the gels were autoradiographed at –80°C using x-ray film. Prestained SDS-PAGE standards were obtained from Bio-Rad (Hercules, CA).

Results

Characterization of CD43 epitopes recognized by HSCA-2 mAb

HSCA-2 mAb resembles the reference CD43 mAb DFT-1 in binding to HeLa cells stably transfected with CD43⁺ cDNA, but not to their mock-transfected (CD43[–]) counterparts (Fig. 1A). HSCA-2 mAb also resembles the DFT-1 mAb in recognizing a neuraminidase-sensitive epitope on KG-1 cells (Fig. 1B). However, although the binding of HSCA-2 mAb to KG-1 cells was all but completely blocked by DFT-1 mAb, the binding of DFT-1 mAb was only ~90% blocked by HSCA-2 mAb even at the highest HSCA-2 mAb concentration (Fig. 1C). These findings may imply that the binding affinity of HSCA-2 mAb is lower than that of DFT-1 mAb. The HSCA-2 mAb immunoprecipitated a surface protein of ~115 kDa in KG-1 cells, whereas DFT-1 mAb immunoprecipitated both the 115-kDa protein and a minor protein with a higher molecular mass of ~125 kDa (Fig. 2A). Immunoprecipitation and blocking experiments with another characterized CD43 mAb, 1G10, confirmed the results with the DFT-1 mAb (data not shown). These results suggest that HSCA-2 mAb reacts with a

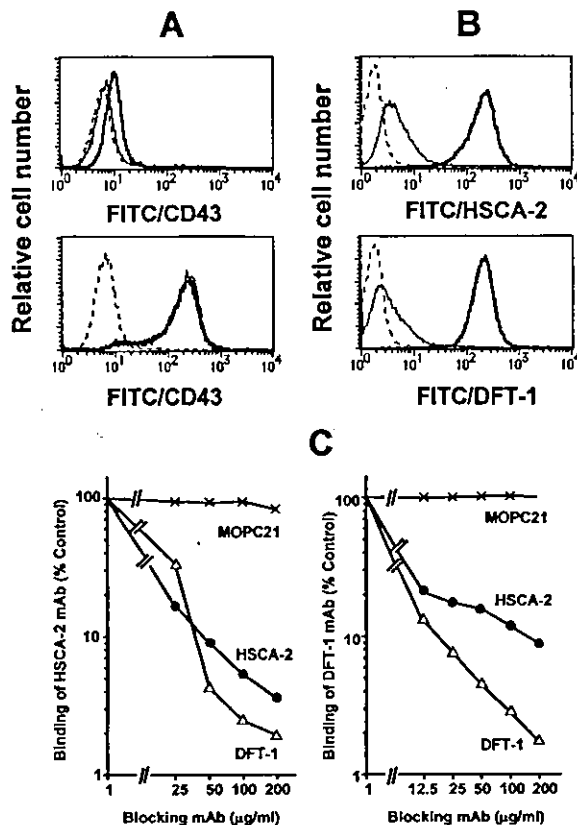


FIGURE 1. Flow cytometric analyses of CD43 expression in CD43⁺ HeLa transfectant and KG-1 cells with HSCA-2 and DFT-1 mAbs. *A*, Direct immunofluorescence staining of mock-transfected (upper panel) and CD43-transfected HeLa cells (lower panel) with FITC-labeled HSCA-2 (thick line), DFT-1 (thin line), and control IgG1 (broken line) mAbs. *B*, Effect of neuraminidase treatment on the expression of CD43 in KG-1 cells. Nontreated (thick line) and treated (thin line) KG-1 cells were stained with FITC-labeled HSCA-2 (upper panel), DFT-1 (lower panel) mAbs. Treated cells also were stained with control IgG1 (broken line). *C*, Blocking of the binding of FITC-labeled HSCA-2 (left) and DFT-1 (right) mAbs to KG-1 cells by excess amounts of HSCA-2, DFT-1, or MOPC21 (IgG1 control) mAbs.

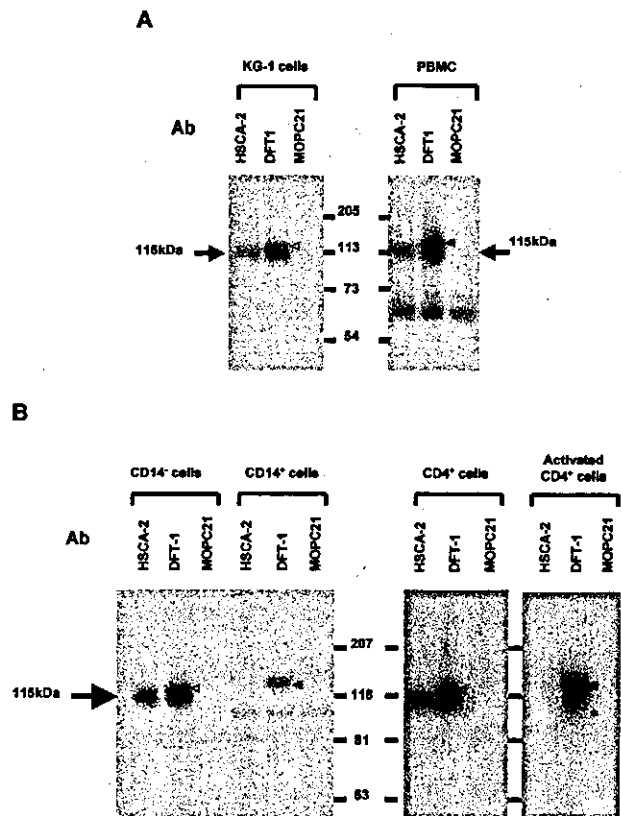


FIGURE 2. Immunoprecipitation of ¹²⁵I-labeled surface proteins from various types of white blood cells with HSCA-2, DFT-1, and MOPC21 (IgG1 control) mAbs. *A*, Immunoprecipitation of KG-1 cells and total PBMCs. *B*, Immunoprecipitation of CD14[–], CD14⁺, CD4⁺, and activated CD4⁺ cells; 105-, 115-, 125-, and 135-kDa protein bands are indicated by an asterisk, arrows, open triangles, and closed triangles, respectively.

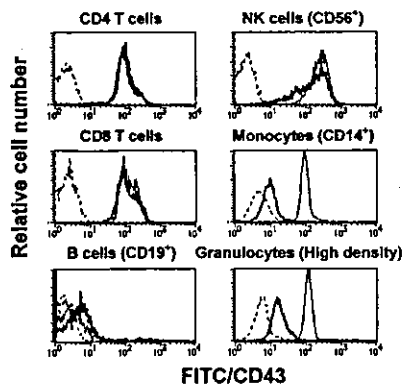


FIGURE 3. Flow cytometric analyses of CD43 expression in peripheral blood cells. For two-color analyses, PBMCs were stained with FITC-labeled HSCA-2 (thick line), DFT-1 (thin line), and control IgG1 (broken line) mAbs in combination with PE-labeled CD4, CD8, CD19, and CD56 mAbs. Monocytes and granulocytes isolated by MACS with CD14 mAb and density centrifugation, respectively, were singly stained with FITC-labeled mAbs. Results are representative of seven different donors.

sialic acid-dependent epitope on the 115-kDa CD43 glycoform in KG-1 cells, but not with its equivalent on the 125-kDa glycoform.

Expression characteristics of CD43 in normal white blood cells

The particular CD43 epitopes recognized by the HSCA-2 or DFT-1 mAb (hereafter abbreviated to CD43(HSCA-2) or CD43(DFT-1)) in normal lymphoid and myeloid cell populations were analyzed by two-color flow cytometry (Fig. 3). The CD43(HSCA-2) and CD43(DFT-1) epitopes were expressed at similar levels in CD4⁺ and CD8⁺ T cell populations. Neither HSCA-2 mAb nor DFT-1 mAb reacted with resting CD19⁺ B cells, whereas they both bound reasonably strongly to either PWM-activated or EBV-transformed B cells (data not shown). The majority of CD56⁺ NK cells expressed both CD43(HSCA-2) and CD43(DFT-1) epitopes at high levels, whereas there was relatively little of the CD43(HSCA-2) epitope in the minor subpopulation of NK cells. DFT-1 mAb was found to bind quite strongly to both purified monocytes and granulocytes, whereas binding by the HSCA-2 mAb was weak enough to be described as nonspecific, as judged by the results of immunoprecipitation analyses (see Fig. 2B). We did not detect any increase in the level of either CD43(HSCA-2) or CD43(DFT-1) in cultured monocytes, even af-

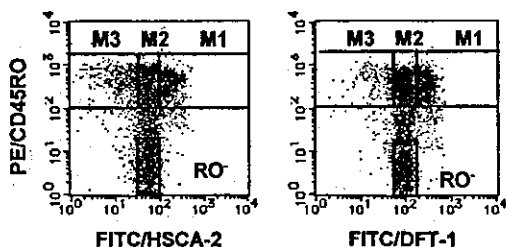


FIGURE 4. Flow cytometric analyses of CD43 expression in CD4⁺ T cell subsets. Expression of CD43 detected by either HSCA-2 (left) or DFT-1 (right) mAbs in combination with CD45RO in CD4⁺ T cells analyzed by triple-color immunofluorescence. Four different subsets were defined within CD4⁺ T cells: CD45RO⁺ cells expressing higher (M1), intermediate (M2), and lower (M3) levels of CD43, and CD45RO⁻ (RO⁻) cells in each CD43 mAb. In each donor a window for the M2 subset was set in a region where the CD43 level detected by each CD43 mAb was from approximately one-half to 2-fold the mean CD43 intensity for RO⁻ cells. Results are representative of six donors.

ter the addition of LPS (data not shown). The HSCA-2 and DFT-1 mAbs both reacted quite strongly with cord blood CD34⁺ cells (data not shown). Two previously used CD43 mAbs, 1G10 and L10, appeared to share the cell type specificities of the DFT-1 mAb (data not shown).

The results of experiments involving immunoprecipitation of ¹²⁵I-labeled surface proteins from PBMCs, CD14⁺ lymphoid cells, and CD4⁺ T cells with CD43 mAbs revealed that the HSCA-2 mAb recognizes only 115-kDa proteins, and whereas the DFT-1 mAb also reacts with 115-kDa proteins it can interact with a second minor, but higher molecular mass (~125 kDa), protein as well (Fig. 2); these findings mirror our previous findings with KG-1 cells (see above). Other findings include the fact that HSCA-2 mAb failed to immunoprecipitate any specific proteins from CD14⁺ monocytes, unlike the DFT-1 mAb, which reacted with a 135-kDa protein (Fig. 2B). In tests with activated CD4⁺ T cells, the DFT-1 mAb immunoprecipitated both the 135-kDa protein and a minor protein with lower molecular mass of 105 kDa, unlike the HSCA-2 mAb, which did not react with proteins of either of these sizes (Fig. 2B). Both the HSCA-2 and DFT-1 mAbs appeared to specifically immunoprecipitate several common, low molecular mass (25- to 40-kDa) proteins in activated CD4⁺ T cells (data not shown).

Expression characteristics of CD43 in CD4⁺ memory T cells

As shown in Fig. 4 (left), the CD4⁺CD45RO⁺ cell population can be divided into three distinct subsets (M1, M2, and M3) on the basis of their CD43(HSCA-2) expression levels; this confirms our previous findings (31). We therefore tried to define the same three subsets on the basis of their CD43(DFT-1) expression levels (Fig. 4, right); interestingly, the proportions of the M1 subset detected with the DFT-1 and HSCA-2 mAbs were not significantly different (Table I), whereas the proportion of the M2 subset defined by the DFT-1 mAb was significantly larger when defined by HSCA-2 mAb, and the proportion of the M3 subset defined by the DFT-1 mAb was significantly smaller than when defined by HSCA-2 mAb. We observed similar subset percentages when the 1G10 and L10 mAbs were used in place of the DFT-1 mAb (Table I). These results indicate that the low levels of CD43(HSCA-2) expression that typify the M3 population do not affect the ability of M3 cells to express other CD43 epitopes.

Accessory functions of CD43 in recall responses of CD4⁺ memory T cells

To analyze possible accessory functions of CD43(HSCA-2) in memory T cells, we first examined the effects of exposure to HSCA-2 mAb on the recall Ag-induced proliferation of total PBMCs in culture. As shown in Fig. 5, HSCA-2 mAb seemed to

Table I. CD4 memory T cell subsets defined by four different CD43 mAbs

CD43 mAb	Subsets (% in total CD4 ⁺ T cells ^a)		
	M1	M2	M3
HSCA-2	19.9 ± 4.4 ^b	21.8 ± 8.0	5.7 ± 3.0
DFT-1	19.0 ± 3.7	25.3 ± 9.4 ^c	3.0 ± 1.4 ^c
L10	20.5 ± 4.3	23.6 ± 8.7 ^c	2.6 ± 1.4 ^c
1G10	19.0 ± 4.1	24.5 ± 8.2 ^c	2.8 ± 1.8 ^c

^a The percentage of each subset in total CD4⁺ T cells was determined by three-color flow cytometry, as shown in Fig. 4A.

^b Average ± SD (n = 6)

^c Value was significantly larger or smaller than that of HSCA-2 mAb by Wilcoxon signed rank test (p < 0.05).

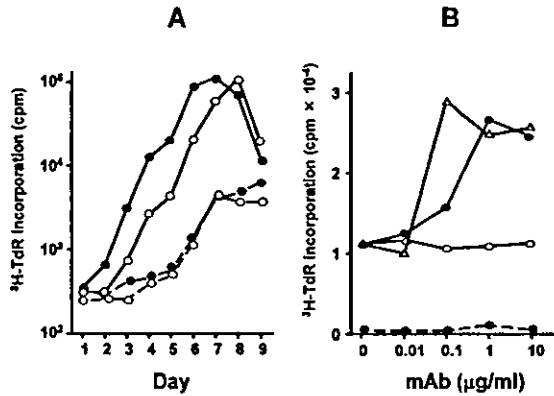


FIGURE 5. Acceleration of proliferative responses of PBMCs to PPD by stimulation with CD43 mAbs. *A*, Time courses of PPD responses. PBMCs were stimulated with (solid line) or without (broken line) PPD (5 µg/ml) in the presence (●) or the absence (○) of HSCA-2 mAb (5 µg/ml). *B*, Dose responses of CD43 mAbs. PBMCs were stimulated with (solid line) or without (broken line) PPD (5 µg/ml) in the presence of HSCA-2 (●), DFT-1 (Δ), and MOPC21 (○) at the various concentrations. Proliferation was measured on day 5 by adding [³H]thymidine during the last 16 h of culture. Results are representative of five donors.

dose-dependently accelerate the proliferation of PPD Ag-stimulated PBMCs, but had no comparable effect on their proliferation in the absence of PPD. The three traditionally used anti-CD43 mAbs (DFT-1 (Fig. 5*B*), and 1G10 and L10 (data not shown)) also proved at least as effective as the HSCA-2 mAb in accelerating PPD-stimulated proliferation of PBMCs. As the majority of PPD-reactive cells appear to be CD4⁺ T cells (data not shown), we examined the effects of the addition of a combination of HSCA-2 mAb and CD28 mAb on the responses of MACS-purified CD4⁺ T cells in the presence of autologous monocytes (Fig. 6). The CD28 mAb that we chose to use in this experiment was the CD28.2 clone, which is capable of strongly costimulating polyclonal T cell responses to plastic- or monocyte-bound CD3 mAb, but (if anything) inhibits Ag-specific responses (39). Thus, whereas HSCA-2 mAb led to a significantly enhanced PPD response in CD4⁺ T cells, the addition of CD28 mAb led to it being slightly inhibited. We also examined the effect of the HSCA-2 mAb on the TT-dependent proliferative response of CD4⁺ T cells and found that it had an enhancing effect (Fig. 6).

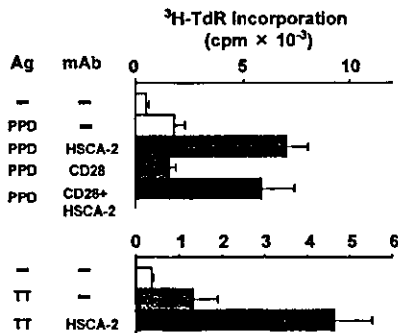


FIGURE 6. Effects of HSCA-2 and CD28 mAbs on the proliferative responses of CD4 T cells to recall Ags. MACS-purified CD4 T cells were stimulated with PPD or TT in the presence of autologous CD14⁺ APC. HSCA-2 (5 µg/ml) and/or CD28 (1 µg/ml) mAbs were added to the culture. Proliferation was measured on day 5 (PPD) or day 7 (TT) by adding [³H]thymidine during the last 16 h of culture. Results were expressed as the mean cpm ± SD and are representative of three donors.

Next we examined the effects of the addition of CD28 and HSCA-2 mAbs on recall responses in each of the three CD4⁺ memory T cell subsets as defined by their separation in a cell sorter on the basis of their CD43(HSCA-2) expression levels (Fig. 4). As shown in Fig. 7*A*, only the M1 subset cells appeared to be capable of responding to PPD; this confirms our previous findings (31). The results of our experiments with the M1 subset mirrored our findings with unseparated CD4⁺ T cell populations, in that the PPD response of M1 subset cells was significantly and dose-dependently enhanced by the addition of HSCA-2 mAb (Fig. 7, *B* and *C*), but was inhibited, rather than enhanced, in the presence of the CD28 mAb (Fig. 7*A*). The PPD responses of the M2 and M3 subset cells were virtually unaffected by the addition of the HSCA-2 mAb (Fig. 7, *B* and *C*). This did not surprise us, given that the M2 and M3 subsets appeared to contain a relatively very

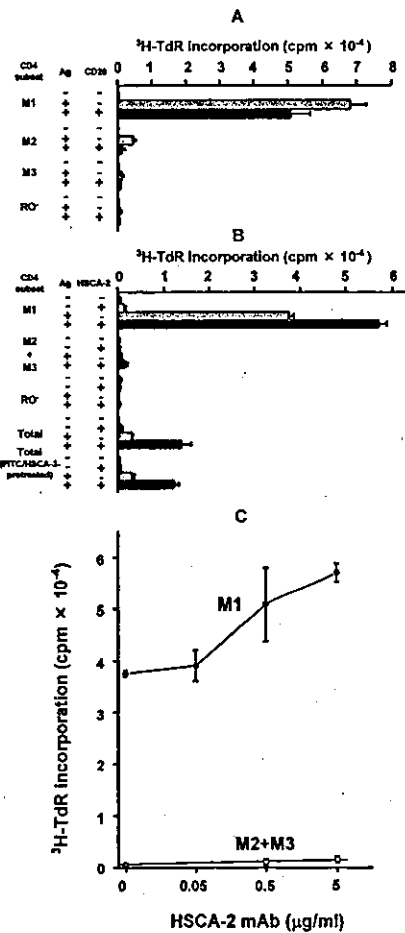


FIGURE 7. Effects of CD28 and HSCA-2 mAbs on the proliferative responses of CD4 T cell subsets to PPD. *A-C*, MACS-purified CD4⁺ T cells were stained with FITC-HSCA-2 and PE-CD45RO mAbs (see Fig. 4*A*, left) and thereafter sorted by FACS into the indicated subsets. Each subset cells and total CD4⁺ T cells were stimulated with PPD in the presence of autologous CD14⁺ APC. CD28 (1 µg/ml; *A*) or HSCA-2 (5 µg/ml; *B*) mAbs were added to the culture. Total CD4⁺ T cells pretreated with FITC-HSCA-2 mAb also were examined for possible effects of immunofluorescence staining with HSCA-2 mAb on the PPD response (*B*). M2+M3, Cell populations sorted by gating the combined region of the M2 and M3 subsets (Fig. 4*A*, left). Dose responses of HSCA-2 mAb for M1 subset cells and a combined cell population of M2 and M3 subsets were examined (*C*). Proliferation was measured on day 5 by adding [³H]thymidine during the last 16 h of culture. Results were expressed as the mean cpm ± SD and are representative of three donors.

small PPD-reactive precursor component (31). The stimulatory effect of the FITC-HSCA-2 mAb that remains attached to cells after its use in the course of their separation was negligible, given that the pretreatment of unseparated CD4⁺ T cells with FITC-HSCA-2 mAb did not significantly alter their subsequent response to PPD, whereas addition of the mAb to cultures of both FITC-HSCA-2 mAb-pretreated and nontreated CD4⁺ T cells increased their responses to PPD to very much the same extent (Fig. 7B). Taken together, the above results indicate that CD43(HSCA-2) is capable of acting as an accessory molecule in the Ag-specific recall response of mature CD4⁺ memory T cells.

Synergistic effects between CD43 and CD28 mAbs in polyclonal response

To determine whether CD43(HSCA-2) can play an accessory role in the polyclonal activation of T cells, we examined the possible effects of the HSCA-2 mAb on the proliferative response of CD4⁺ T cells to monocyte-bound CD3 mAb (Fig. 8). We found that the

HSCA-2 mAb did have an effect, but that it was only marginally costimulatory at lower (0.001–0.1 μg/ml) CD3 mAb concentrations and that its effectiveness disappeared at the highest concentration tested (1 μg/ml). Interestingly, the results shown in Fig. 8A provide convincing evidence that the CD28/HSCA-2 mAb combination had a synergistic effect on the CD3 mAb-mediated polyclonal response (Fig. 8A). A similar synergistic effect on the CD3-mediated response was observed when the mAbs involved were DFT-1 and CD28 (data not shown).

Cells of two of the three CD4⁺ memory T cell subsets (M1 and M2) responded strongly to monocyte-bound CD3 mAb, whereas M3 subset cells did not (Fig. 8B). These findings are in agreement with those in our original report (31). The HSCA-2 mAb was almost as effective as CD28 mAb in their enhancement of polyclonal responses in M1 and M2 subset cells, but had no such effect in M3 subset cells. There were marginal synergistic effects on polyclonal responses when M1 and M2 subset cells were cotreated with the HSCA-2 and CD28 mAbs, although a much more obvious synergistic effect became evident when we used RO⁺ naive subset cells instead.

When the Fab portion of the HSCA-2 mAb was used instead of intact Ab, we could see no indication of either an enhanced PPD-mediated stimulatory response or a synergistic interaction involving the CD28 mAb and CD3 mAb polyclonal responses (data not shown).

Discussion

HSCA-2 mAb specifically recognizes a neuraminidase-sensitive epitope on the low molecular mass (115-kDa) glycoform of the CD43 molecule that is predominantly expressed in lymphoid cells, including resting T and NK cells. By contrast, all previously described CD43 mAbs (including the DFT-1 mAb) react strongly or even very strongly with a larger (135-kDa) CD43 glycoform that is expressed in myeloid cells such as monocytes and granulocytes. Importantly, the HSCA-2 mAb does not appear to recognize the 135-kDa glycoform and hence binds only marginally, if at all, to myeloid cells; it also does not immunoprecipitate a third high molecular mass (125-kDa) CD43 protein that is recognized by the DFT-1mAb in both KG-1 and CD4⁺ T cells. Taken together, these findings suggest that the HSCA-2 mAb is specific for a novel glycoepitope on the 115-kDa glycoform of CD43.

Interestingly, HSCA-2 mAb differs from all pre-existing CD43 mAbs in being unable to recognize the high molecular mass CD43 glycoform (135 kDa) that is present on activated CD4⁺ T cells. Thus, the 135-kDa CD43 glycoform consists of a more fully glycosylated version that is generated in the course of the increase in molecular mass of the 115-kDa CD43 glycoform that occurs during T cell activation (5, 7); it is possible that the HSCA-2 glycoepitope is either lost or masked in the course of this glycosyl modification process. As the molecular mass of the CD43 polypeptide is ~40 kDa, the 25- to 40-kDa proteins recognized by HSCA-2 mAb in activated T cells could well be degradation forms of CD43, and we have even observed what appeared to be the gradual disappearance of CD43(HSCA-2) epitopes from a subpopulation of activated CD4⁺CD45RO⁺ T cells (manuscript in preparation).

We noticed that there were significant differences in the distribution of the CD4 memory T cell subsets depending upon which of the available CD43 mAbs was used in their separation. Thus, for example, the percentages of M2 subset cells that we observed in separations achieved using the HSCA-2 mAb were significantly smaller than those observed in separations using any of the other available mAbs. In the case of the M3 subsets, the percentages were larger with the HSCA-2 mAb than with any of the others. These CD43 mAb-dependent differences in subset distributions

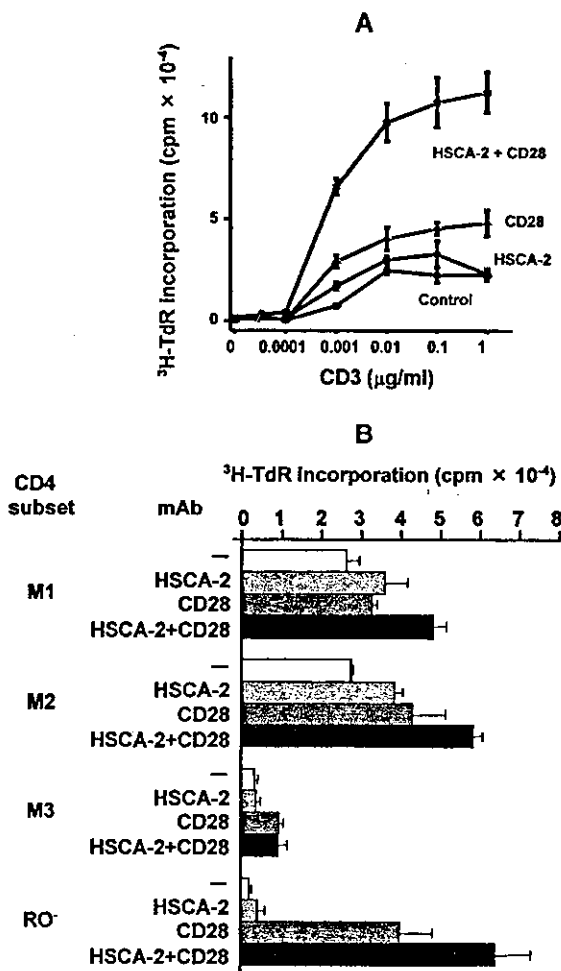


FIGURE 8. Synergistic effects of HSCA-2 and CD28 mAbs on the proliferative responses of CD4⁺ T cells to monocyte-bound CD3 mAb. Total CD4⁺ T cells (A) and CD4⁺ T cell subset cells (B) were stimulated with various concentrations (A) or 0.1 μg/ml (B) of CD3 mAb in the presence of autologous CD14⁺ monocytes. The effects of HSCA-2 (5 μg/ml) and CD28 (1 μg/ml) mAbs on the CD3 responses were tested by single or combined use of these mAbs. Proliferation was measured on day 3 by adding [³H]thymidine during the last 16 h of culture. Results were expressed as the mean cpm ± SD and are representative of three donors.

may correspond to differences in such subset cell functions as memory vs anergy, but we have yet to explore this possibility in any detail.

In this report we show that HSCA-2 and certain other CD43 mAbs are capable of accelerating both the recall Ag-induced and CD3 mAb-induced proliferation of CD4 memory T cells. There are previous reports indicating that CD43 molecules may also have accessory involvements in T cell activation, such as, for example, in mice, where CD43 mAb appears to costimulate T cell activation during treatment with plastic-bound CD3 mAb and alloantigens (17, 40). In humans, however, there does not appear to be any evidence of CD43 mAb being involved in a costimulatory capacity in the polyclonal activation of T cells (41). In situations involving Ag-specific responses, there is one report that CD43 is necessary for the production of IL-2 in HLA class II-specific human hybridoma T cells (42), but it is important to note that the experimental system used to obtain these data was an unusually artificial one. There are, however, several publications in which it is claimed that a number of CD43 mAbs can stimulate Ag-independent human T cell proliferation in a multicomponent test system that requires the presence of CD43-stimulated monocytes (43–46). Thus, the results described in this study appear to provide the first evidence that T cell-determined CD43 may help to stimulate the Ag-specific proliferative responses of freshly isolated T cells in humans. In the case of our new mAb (HSCA-2), we can exclude any involvement of CD43-mediated monocyte stimulation in T cell activation. The reason why HSCA-2 mAb differs from all previously used CD43 mAbs in this important way is that it appears to lack reactivity to the 135-kDa CD43 glycoform expressed in monocytes.

Given the above consideration, it seems reasonable to assume that CD43 plays a part in some of the cell signaling events that are likely to be involved in memory T cell activation. Up-regulated expression of CD43 in M1 subset cells may cause an increase in activation signaling in concert with other up-regulated costimulatory molecules such as CD28 (31). Our observation that CD43 and CD28 mAbs act synergistically to stimulate the polyclonal response of CD4⁺ T cells to anti-CD3 mAb may indicate that both CD43 and CD28 have an accessory signaling role in the induction of the polyclonal response. It has previously been reported that T cell activation through CD43 cross-linking in humans induces serine phosphorylation of Cbl proteins and tyrosine phosphorylation of Vav (19, 20). It has also been reported that one of the CD28-determined costimulatory signaling processes is mediated by tyrosine phosphorylation of Vav1, which is, in turn, negatively regulated by Cbl-b (47–49). Thus, although the precise molecular mechanisms underlying the costimulatory effects of CD43 remain to be determined, it is possible that both CD28 and CD43 are capable of synergistically enhancing the activation of CD4⁺ memory T cells by a mechanism involving the common signaling pathway.

Acknowledgments

We are grateful to Dr. Donald MacPhee for his valuable suggestions, to Mika Yamaoka for her excellent assistance with FACS analysis, and to Mika Yonezawa and Jeffrey Hart for manuscript preparation.

References

- Remold-O'Donnell, E. 1995. CD43 cluster report. In *Leucocyte Typing*. Vol. V: *White Cell Differentiation Antigens*. S. F. Schlossman, L. Boumsell, W. Gilks, J. M. Harlan, T. Kishimoto, C. Morimoto, J. Ritz, S. Shaw, R. Silverstein, T. Springer, et al., eds. Oxford University Press, New York, p. 1697.
- Rosenstein, Y., A. Santana, and G. Pedraza-Alva. 1999. CD43, a molecule with multiple functions. *Immunol. Res.* 20:89.
- Cyster, J. G., D. M. Shotton, and A. F. Williams. 1991. The dimensions of the T lymphocyte glycoprotein leukosialin and identification of linear protein epitopes that can be modified by glycosylation. *EMBO J.* 10:893.
- Carlsson, S. R., H. Sasaki, and M. Fukuda. 1986. Structural variations of O-linked oligosaccharides present in leukosialin isolated from erythroid, myeloid, and T-lymphoid cell lines. *J. Biol. Chem.* 261:12787.
- Piller, F., F. Le Deist, K. I. Weinberg, R. Parkman, and M. Fukuda. 1991. Altered O-glycan synthesis in lymphocytes from patients with Wiskott-Aldrich syndrome. *J. Exp. Med.* 173:1501.
- Jones, A. T., B. Federspiel, L. G. Ellies, M. J. Williams, R. Burgener, V. Duronio, C. A. Smith, F. Takei, and H. J. Ziltener. 1994. Characterization of the activation-associated isoform of CD43 on murine T lymphocytes. *J. Immunol.* 153:3426.
- Piller, F., V. Piller, R. I. Fox, and M. Fukuda. 1988. Human T-lymphocyte activation is associated with changes in O-glycan biosynthesis. *J. Biol. Chem.* 263:15146.
- Harrington, L. E., M. Galvan, L. G. Baum, J. D. Altman, and R. Ahmed. 2000. Differentiating between memory and effector CD8 T cells by altered expression of cell surface O-glycans. *J. Exp. Med.* 191:1241.
- Onami, T. M., L. E. Harrington, M. A. Williams, M. Galvan, C. P. Larsen, T. C. Pearson, N. Manjunath, L. G. Baum, B. D. Pearce, and R. Ahmed. 2002. Dynamic regulation of T cell immunity by CD43. *J. Immunol.* 168:6022.
- Ostberg, J. R., R. K. Barth, and J. G. Frelinger. 1998. The Roman god Janus: a paradigm for the function of CD43. *Immunol. Today* 19:546.
- Manjunath, N., M. Correa, M. Ardman, and B. Ardman. 1995. Negative regulation of T-cell adhesion and activation by CD43. *Nature* 377:535.
- Stockton, B. M., G. Cheng, N. Manjunath, B. Ardman, and U. H. von Andrian. 1998. Negative regulation of T cell homing by CD43. *Immunity* 8:373.
- McEvoy, L. M., H. Sun, J. G. Frelinger, and E. C. Butcher. 1997. Anti-CD43 inhibition of T cell homing. *J. Exp. Med.* 185:1493.
- Woodman, R. C., B. Johnston, M. J. Hickey, D. Teoh, P. Reinhardt, B. Y. Poon, and P. Kubers. 1998. The functional paradox of CD43 in leukocyte recruitment: a study using CD43-deficient mice. *J. Exp. Med.* 188:2181.
- He, Y. W., and M. J. Bevan. 1999. High level expression of CD43 inhibits T cell receptor/CD3-mediated apoptosis. *J. Exp. Med.* 190:1903.
- Brown, T. J., W. W. Shuford, W. C. Wang, S. G. Nadler, T. S. Bailey, H. Marquardt, and R. S. Mittler. 1996. Characterization of a CD43/leukosialin-mediated pathway for inducing apoptosis in human T-lymphoblastoid cells. *J. Biol. Chem.* 271:27686.
- Sperling, A. I., J. M. Green, R. L. Mosley, P. L. Smith, R. J. DiPaolo, J. R. Klein, J. A. Bluestone, and C. B. Thompson. 1995. CD43 is a murine T cell costimulatory receptor that functions independently of CD28. *J. Exp. Med.* 182:139.
- Pedraza-Alva, G., L. B. Merida, S. J. Burakoff, and Y. Rosenstein. 1996. CD43-specific activation of T cells induces association of CD43 to Fyn kinase. *J. Biol. Chem.* 271:27564.
- Pedraza-Alva, G., L. B. Merida, S. J. Burakoff, and Y. Rosenstein. 1998. T cell activation through the CD43 molecule leads to Vav tyrosine phosphorylation and mitogen-activated protein kinase pathway activation. *J. Biol. Chem.* 273:14218.
- Pedraza-Alva, G., S. Sawasdikosol, Y. C. Liu, L. B. Merida, M. E. Cruz-Munoz, F. Ocegueda-Yanez, S. J. Burakoff, and Y. Rosenstein. 2001. Regulation of Cbl molecular interactions by the co-receptor molecule CD43 in human T cells. *J. Biol. Chem.* 276:729.
- Thurman, E. C., J. Walker, S. Jayaraman, N. Manjunath, B. Ardman, and J. M. Green. 1998. Regulation of in vitro and in vivo T cell activation by CD43. *Int. Immunol.* 10:691.
- Carlow, D. A., S. Y. Corbel, and H. J. Ziltener. 2001. Absence of CD43 fails to alter T cell development and responsiveness. *J. Immunol.* 166:256.
- Allenspach, E. J., P. Cullinan, J. Tong, Q. Tang, A. G. Tesciuba, J. L. Cannon, S. M. Takahashi, R. Morgan, J. K. Burkhardt, and A. I. Sperling. 2001. ERM-dependent movement of CD43 defines a novel protein complex distal to the immunological synapse. *Immunity* 15:739.
- Delon, J., K. Kaibuchi, and R. N. Germain. 2001. Exclusion of CD43 from the immunological synapse is mediated by phosphorylation-regulated relocation of the cytoskeletal adaptor moesin. *Immunity* 15:691.
- Shaw, A. S. 2001. FERMIing up the synapse. *Immunity* 15:683.
- Stoll, S., J. Delon, T. M. Brotz, and R. N. Germain. 2002. Dynamic imaging of T cell-dendritic cell interactions in lymph nodes. *Science* 296:1873.
- Cullinan, P., A. I. Sperling, and J. K. Burkhardt. 2002. The distal pole complex: a novel membrane domain distal to the immunological synapse. *Immunol. Rev.* 189:111.
- Savage, N. D., S. L. Kimzey, S. K. Bromley, K. G. Johnson, M. L. Dustin, and J. M. Green. 2002. Polar redistribution of the sialoglycoprotein CD43: implications for T cell function. *J. Immunol.* 168:3740.
- Yousefi-Etamad, R., and B. Axelsson. 1996. Parallel pattern of expression of CD43 and of LFA-1 on the CD45RA⁺ (naive) and CD45RO⁺ (memory) subsets of human CD4⁺ and CD8⁺ cells: correlation with the aggregative response of the cells to CD43 monoclonal antibodies. *Immunology* 87:439.
- Mukasa, R., T. Homma, T. Ohtsuki, O. Hosono, A. Souta, T. Kitamura, M. Fukuda, S. Watanabe, and C. Morimoto. 1999. Core 2-containing O-glycans on CD43 are preferentially expressed in the memory subset of human CD4 T cells. *Int. Immunol.* 11:259.
- Ohara, T., K. Koyama, Y. Kusunoki, T. Hayashi, N. Tsuyama, Y. Kubo, and S. Kyoizumi. 2002. Memory functions and death proneness in three CD4⁺CD45RO⁺ human T cell subsets. *J. Immunol.* 169:39.
- Sallusto, F., D. Lenig, R. Forster, M. Lipp, and A. Lanzavecchia. 1999. Two subsets of memory T lymphocytes with distinct homing potentials and effector functions. *Nature* 401:708.
- Kyoizumi, S., M. Akiyama, N. Kouno, K. Kobuke, M. Hakoda, S. L. Jones, and M. Yamakido. 1985. Monoclonal antibodies to human squamous cell carcinoma of the lung and their application to tumor diagnosis. *Cancer Res.* 45:3274.

34. Andrew, S. M., and J. Titus. 1996. Fragmentation of immunoglobulin G. In *Current Protocols in Immunology*. J. E. Coligan, A. M. Kruisbeek, D. H. Margulies, E. M. Shevach, and W. Strober, eds. John Wiley & Sons, New York and London, p. 2. 10.
35. Nunes, J., S. Klasen, M. Ragueneau, C. Pavon, D. Couez, C. Mawas, M. Bagnasco, and D. Olive. 1993. CD28 mAbs with distinct binding properties differ in their ability to induce T cell activation: analysis of early and late activation events. *Int. Immunol.* 5:311.
36. Remold-O'Donnell, E., D. M. Kenney, R. Parkman, L. Cairns, B. Savage, and F. S. Rosen. 1984. Characterization of a human lymphocyte surface sialoglycoprotein that is defective in Wiskott-Aldrich syndrome. *J. Exp. Med.* 159:1705.
37. Horejsi, V., and H. Stockinger. 1997. CD43 workshop panel report. In *Leucocyte Typing*, Vol. VI: *White Cell Differentiation Antigens*. T. Kishimoto, H. Kikutani, A. E. G. Kr. von dem Borne, S. M. Goyert, D. Y. Mason, M. Miyasaka, L. Moretta, K. Okumura, S. Shaw, T. A. Springer, et al., eds. Garland, New York and London, p. 494.
38. Kyoizumi, S., M. Akiyama, Y. Hirai, Y. Kusunoki, K. Tanabe, and S. Umeki. 1990. Spontaneous loss and alteration of antigen receptor expression in mature CD4⁺ T cells. *J. Exp. Med.* 171:1981.
39. Olive, D., C. Cerdan, R. Costello, I. Sielleur, M. Ragueneau, F. Pages, S. Klasen, J. Nunes, and J. Imbert. 1995. CD28 and CTLA-4 cluster report. In *Leucocyte Typing*, Vol. V: *White Cell Differentiation Antigens*. S. F. Schlossman, L. Boumsell, W. Gilks, J. M. Harlan, T. Kishimoto, C. Morimoto, J. Ritz, S. Shaw, R. Silverstein, T. Springer, et al., ed. Oxford University Press, New York, p. 360.
40. Walker, J., and J. M. Green. 1999. Structural requirements for CD43 function. *J. Immunol.* 162:4109.
41. Tkaczuk, J., T. Al Saati, I. Escargueil-Blanc, A. Salvayre, V. Horejsi, M. Durand, C. de Preval, E. Ohayon, G. Delsol, and M. Abbal. 1999. The CBF.78 monoclonal antibody to human sialophorin has distinct properties giving new insights into the CD43 marker and its activation pathway. *Tissue Antigens* 54:1.
42. Park, J. K., Y. J. Rosenstein, E. Remold-O'Donnell, B. E. Bierer, F. S. Rosen, and S. J. Burakoff. 1991. Enhancement of T-cell activation by the CD43 molecule whose expression is defective in Wiskott-Aldrich syndrome. *Nature* 350:706.
43. Mentzer, S. J., E. Remold-O'Donnell, M. A. Crimmins, B. E. Bierer, F. S. Rosen, and S. J. Burakoff. 1987. Sialophorin, a surface sialoglycoprotein defective in the Wiskott-Aldrich syndrome, is involved in human T lymphocyte proliferation. *J. Exp. Med.* 165:1383.
44. Axelsson, B., R. Youseffi-Etemad, S. Hammarstrom, and P. Perlmann. 1988. Induction of aggregation and enhancement of proliferation and IL-2 secretion in human T cells by antibodies to CD43. *J. Immunol.* 141:2912.
45. Nong, Y. H., E. Remold-O'Donnell, T. W. LeBien, and H. G. Remold. 1989. A monoclonal antibody to sialophorin (CD43) induces homotypic adhesion and activation of human monocytes. *J. Exp. Med.* 170:259.
46. Alvarado, M., C. Klassen, J. Cemy, V. Horejsi, and R. E. Schmidt. 1995. MEM-59 monoclonal antibody detects a CD43 epitope involved in lymphocyte activation. *Eur. J. Immunol.* 25:1051.
47. Chiang, Y. J., H. K. Kole, K. Brown, M. Naramura, S. Fukubara, R. J. Hu, I. K. Jang, J. S. Gutkind, E. Shevach, and H. Gu. 2000. Cbl-b regulates the CD28 dependence of T-cell activation. *Nature* 403:216.
48. Bachmaier, K., C. Krawczyk, I. Kozieradzki, Y. Y. Kong, T. Sasaki, A. Oliveira-dos-Santos, S. Mariathasan, D. Bouchard, A. Wakeham, A. Itie, et al. 2000. Negative regulation of lymphocyte activation and autoimmunity by the molecular adaptor Cbl-b. *Nature* 403:211.
49. Krawczyk, C., K. Bachmaier, T. Sasaki, G. R. Jones, B. S. Snapper, D. Bouchard, I. Kozieradzki, S. P. Ohashi, W. F. Alt, and M. J. Penninger. 2000. Cbl-b is a negative regulator of receptor clustering and raft aggregation in T cells. *Immunity* 13:463.

Decreases in Percentages of Naïve CD4 and CD8 T Cells and Increases in Percentages of Memory CD8 T-Cell Subsets in the Peripheral Blood Lymphocyte Populations of A-Bomb Survivors

Mika Yamaoka,^a Yoichiro Kusunoki,^{a,1} Fumiyoshi Kasagi,^b Tomonori Hayashi,^a Kei Nakachi^a and Seishi Kyoizumi^a

Departments of ^aRadiobiology/Molecular Epidemiology and ^bEpidemiology, Radiation Effects Research Foundation, Hiroshima, Japan

Yamaoka, M., Kusunoki, Y., Kasagi, F., Hayashi, T., Nakachi, K. and Kyoizumi, S. Decreases in Percentages of Naïve CD4 and CD8 T Cells and Increases in Percentages of Memory CD8 T-Cell Subsets in the Peripheral Blood Lymphocyte Populations of A-Bomb Survivors. *Radiat. Res.* 161, 290–298 (2004).

Our previous studies have revealed a clear dose-dependent decrease in the percentage of naïve CD4 T cells that are phenotypically CD45RA⁺ in PBL among A-bomb survivors. However, whether there is a similar radiation effect on CD8 T cells has remained undetermined because of the unreliability of CD45 isoforms as markers of naïve and memory subsets among the CD8 T-cell population. In the present study, we used double labeling with CD45RO and CD62L for reliable identification of naïve and memory cell subsets in both CD4 and CD8 T-cell populations among 533 Hiroshima A-bomb survivors. Statistically significant dose-dependent decreases in the percentages of CD45RO⁻/CD62L⁺ naïve cells were found in the CD8 T-cell population as well as in the CD4 T-cell population. Furthermore, the percentages of CD45RO⁺/CD62L⁺ and CD45RO⁺/CD62L⁻ memory T cells were found to increase significantly with increasing radiation dose in the CD8 T-cell population but not in the CD4 T-cell population. These results suggest that the prior A-bomb exposure has induced long-lasting deficits in both naïve CD4 and CD8 T-cell populations along with increased proportions of these particular subsets of the memory CD8 T-cell population. © 2004

by Radiation Research Society

INTRODUCTION

T-cell homeostasis is achieved by the balance between renewal and death among naïve and memory T cells, and maintenance of both naïve and memory T-cell pools is important for the body to protect itself against intrusions by pathogens (1). Exposure to radiation is thought to affect T-cell homeostasis, but little is known about the effects of

radiation on the naïve and memory T-cell pools and their relationship to disease development (2–4), even though increased risks of various diseases including infectious (5) and autoimmune diseases (6) are still observed among A-bomb survivors. Our study therefore aimed to clarify whether the previous radiation exposure might have brought about a perturbation of T-cell homeostasis involving maintenance of normal-sized pools of both naïve and memory T cells.

Our previous studies clearly indicated that the percentages of CD4 (helper) T cells, especially those of CD45RA⁺ (naïve) CD4 T cells, decreased in the PBL of A-bomb survivors; the decrease depended on the radiation dose (3, 7). The radiation sensitivity of CD4 and CD8 (cytotoxic) T cells *ex vivo* is approximately equal (8). In addition, the majority of CD4 and CD8 T cells are produced in the thymus by the same precursor thymocytes, CD4⁺/CD8⁺ cells (9). Thus it could be assumed that A-bomb radiation would induce similar damage to peripheral naïve CD4 and CD8 T-cell populations and that the recovery of these T-cell populations would be very similar. However, the question still remained as to the long-term effects of radiation on the recovery of naïve CD8 T-cell populations because of the unreliability of expression of CD45 isoform expression for markers of naïve CD8 T-cell populations. Several studies have proven that the CD45RA⁺ (i.e. CD45RO⁻) fraction of the CD8 T-cell population contains some cells that do not express the lymph node homing receptor, CD62L (L-selectin), and that these cells exhibit effector T-cell functions (10–14). Further indications from these studies are that naïve CD8 T-cell populations the CD45RA⁺(CD45RO⁻) cell fraction can be separated precisely by analyzing their CD62L expression status. In the present study, we conducted three-color flow cytometry using a combination of CD8, CD45RO and CD62L monoclonal antibodies (mAbs) to specifically enumerate the naïve and memory CD8 T-cell populations of A-bomb survivors. The percentages of CD45RO⁻/CD62L⁺ (naïve) CD8 T cells were found to decrease dose-dependently in the PBL of the survivors, indicating that the naïve T-cell pools are poorly maintained not only in the CD4 but also in the CD8 T-cell populations

¹ Address for correspondence: Department of Radiobiology/Molecular Epidemiology, Radiation Effects Research Foundation, 5-2 Hijiyama Park, Minami-ku, Hiroshima, 732-0815 Japan; e-mail: ykusunok@rerf.or.jp.